Contaminant Formation and Mobilization in Water Due to Fire Events

A Major Qualifying Project
Submitted to the Faculty of
WORCESTER POLYTECHNIC INSTITUTE
in partial fulfillment of the requirements for the
Degree of Bachelor of Science

in
Chemical Engineering, Civil Engineering, Environmental Engineering, Mechanical Engineering
and Chemistry

Submitted by Lisa Cristiano, Drew Grenier, Rayna Harter, Logan O'Donnell, Nihal Patel
Matthew Penkala, Isabelle Rhodes, Alexandra Scariati, and Avery Vreeland

Date: April 22, 2022

Report Submitted to:
Professor John Bergendahl
Professor Ali S. Rangwala
Professor James P. Dittami
Professor Jagannath Jayachandran
Raymond Ranellone
Worcester Polytechnic Institute

`

Acknowledgements

`

Abstract

This report analyzes contaminant mobilization in water as a result of structure fire events through four objectives: identify common materials involved in these fire events, develop a standardized burn method for these materials, develop a method to analyze water samples, and identify the contaminants and their concentrations. To accomplish these objectives fuel packages composed of white pine wood, high-density polyethylene (HDPE), chemical resistant polyvinyl chloride (PVC), and neoprene rubber were constructed. Fuel packages were burned and suppressed with water. The water used for fire suppression was collected and analyzed using Gas Chromatography-Mass Spectrometry (GC-MS) to determine contaminant concentrations in each water sample. This project found that all eight water samples contained benzene, pyrene and naphthalene, and the samples from one of the rubber cribs contained o-xylene. This is consistent with the expected results, but the detected concentrations were lower than literature reported values.

`

Capstone Design Statement

The Accreditation Board for Engineering and Technology (ABET) requires all students in an accredited engineering program to complete a capstone design experience prior to obtaining their engineering degree. Throughout a capstone design experience, students apply knowledge acquired through previous coursework, projects, and studies to successfully address the goal and objectives of their design experience. The capstone design experience at Worcester Polytechnic Institute is completed through the Major Qualifying Project (MQP).

This MQP demonstrates the use of design processes for the development of a crib suppression system that incorporates a number of structural and mechanical components into its design to accomplish the end goal of identification of contaminants produced from the thermal degradation of common infrastructure materials.

The structural design of each crib was developed using extensive empirical research on the correlation between crib composition and crib burning rate. The primary components of a crib's design that affected the average burning rate were the following: varying the spacing between sticks, the number of sticks, and the size of the sticks. These parameters heavily influenced the final determination of our crib dimensions. Encouraging a sufficient radiative heat exchange between wood and polymer fuel elements was also imperative to the design process. The spacing between these elements and the ratio of wood to polymers was a large factor in accounting for a sufficient radiative heat exchange, and ultimately promoting the amount of contaminants potentially mobilized by our polymer fuel elements during suppression.

The suppression system's design was instrumental to the effectiveness of our experiment. To ensure contaminant mobilization during suppression, our fires had to be suppressed, and not extinguished fully. This is a unique challenge for water application as simply spraying the fire with a mist would be inconsistent between trials and would not give us the required amount of water to test for contaminants with water samples. A suppression system was constructed that allowed our team to adjust the flow rate of the water suppressing the fire, as well as evenly distribute the water to each crib between trials. Based on the calculated heat release rate of a

`

4x4x3.75 inch pine wood crib, a flow rate of 6-600 ml/min was determined to successfully suppress and not extinguish each crib.

Trial burns were conducted to test the steady-state burn rate and steady-state burning duration for each of our cribs. This information allowed us to calculate the amount of water expected during suppression for each crib composition.

Once the water from the fire suppression was collected, a vacuum pump filtration system was designed to filter out the ash and soot collected in the samples. A vacuum pump was attached to a flask containing a funnel and .45 μm glass fiber filter membrane. The pump was turned on and each sample was slowly poured through the filter membrane. This allowed for the collection of the insoluble debris to avoid damaging the Gas Chromatograph-Mass Spectrometer (GC-MS).

To finish preparing the samples for the GC-MS, a solid phase extraction (SPE) process was designed. Four SPE cartridges were set up at a time, which were attached to a vacuum pump and tubes to siphon the samples through. These cartridges were pretreated with methylene chloride and purified water. The 50 mL samples were then run through the SPE cartridge at a speed of 1 mL/minute. After each sample was completely run through a cartridge, new test tubes were placed underneath the cartridge and 4 mL of methylene chloride was used to elute the cartridge. This design allowed for 4 mL samples to be prepared for each of eight test burns, which were then ready to run through the GC-MS.

`

Professional Licensure Statement

The National Council of Examiners for Engineering and Surveying (NCEES) presides over the evaluation for Professional Engineering (PE) Lisensurship to ensure all engineers are held to equally high standards. As a PE, individuals are expected to uphold the health, safety, and wellbeing of those affected by their work. In the position of a PE, individuals are granted the privilege and requirement of signing, sealing, and approving engineering plans prior the execution of a project.

The process of acquiring a PE begins with graduating from a four-year ABET-accredited engineering program or by having four years of engineering experience that is satisfactory to the Board of Engineering. The second step is passing the Fundamentals of Engineering (FE) exam, wherein an individual becomes an Engineer in Training (EIT). As an EIT, candidates must work under the direct supervision of a PE for at least four years, as required by the National Society of Professional Engineers. Here individuals will be exposed to various engineering practices, skills, and insight, in order to develop a comprehensive portfolio of their work, which will later be submitted to the PE board for approval. Following approval of a candidate's portfolio, the candidate's next step towards licensure is passing the PE exam, which is administered by each state's board. It should be noted that employers often prefer that individuals take the FE prior to employment to encourage PE licensure later on. Once an individual has obtained their PE, they are now open to further growth and authority in the workplace. Moreover, a PE license allows an individual to branch out and begin their own private engineering firm—if interested. A PE license is retained through an individual's consistent proficiency and development of professional skills.

`

Authorship

Each member of this team played a significant role in developing each of the finalized chapters and sections of this report. Whether it was through the process of outlining, writing, researching, editing, organizing, performing lab work, or formatting, everyone was a leader in their own right over the course of this project. Team members complemented each other's strengths and weaknesses and were willing to lend a helping hand or assist in other member's portions of the project.

`

Executive Summary

Introduction

Wildfires and structural fires have increased in number and intensity over the past decade; the publicity surrounding these events has increased as well. These events are predicted to continue to increase in frequency in the coming decades, due to the effects of climate change. Also the effects of runoff that occurs as a result of fire suppression is unknown. This is especially true of structural fires, because the effects of potentially mobilized contaminants on surrounding water bodies, on other areas of the environment, and on human health, is unknown. Due to the ongoing effects of climate change, potential mitigation strategies and the analysis of both short- and long-term contamination effects will be necessary for future communities. Research was conducted with the following objectives: identify common materials involved in these fire events; develop a standardized burn method for these materials; and develop a method to analyze water samples to identify the contaminants and their concentrations.

Background

Recently, there have been record-breaking numbers of structural fires across the United States, requiring large quantities of water for suppression efforts. While efficient in extinguishing fires, the water used becomes polluted with contaminants through various combustion reactions and mass transfer to water. The runoff of this contaminated water can seep into local water systems and into sources of drinking water, such as water distribution mains. This has the potential to harm ecosystems and human health.

Several case studies from the most recent California fire events have demonstrated the impacts of contamination as a result of the thermal degradation of plastics and other materials. Several toxic chemicals have been documented during the burning of high-density polyethylene (HDPE), polyvinyl chloride (PVC), and neoprene rubber within water suppression samples.

Published research has been limited to water and air contamination from wildfires and air contamination from residential fires. Additionally, water contamination analysis has been limited to identification and not quantification of these contaminants.

`

Methodology

To accomplish the objectives of this research, a fuel package was constructed that would release sufficient radiant flux to thermally degrade selected burn materials. A crib structure was designed and four materials—HDPE, chemical resistant PVC, neoprene rubber, and white pine wood—were selected. Burns were conducted to generate steady-state curves with and without water suppression. All trials were then performed using a consistent burn method, suppressed after steady state was observed, and water was collected for analysis.

Each water sample was prepared using vacuum filtration, solid phase extraction, and elution with methylene chloride. Gas Chromatography-Mass Spectrometry (GC-MS) was used to quantify and identify contaminants. Quantification was completed using standard curves generated with Supelco EPA 625 Semivolatile Calibration Mix and Supelco EPA 502/524 Volatiles Organic Calibration Mix standards. Benzene, o-xylene, pyrene, naphthalene, anthracene and ethylbenzene were selected as indicator contaminants. The samples were then analyzed with GC-MS to identify these contaminants, providing results for each experimental burn.

Results and Discussion

During the preliminary steady-state combustion trials, the average duration of the steady state of the fire lasted 100 seconds, while the average mass loss rate during steady state across all cribs was 0.66 g/s. Once suppression was initiated, there was a period of a few seconds where the mass loss rate dropped rapidly due to the application of water, and was followed by fluctuating mass loss rates for the duration of the burn. During this period, each crib burned at a distinctly steady and less intense burning rate until suppression was stopped. Each crib burned away approximately 90-100 grams of material, aside from HDPE, which lost more mass. Similarly, each crib amassed a similar amount of water on their surface areas after suppression except for HDPE, which accumulated significantly less water. Fuel package materials change their nature depending on their material classification—such as their flash point or whether they are

`

thermoset or thermoplastic—affecting both steady state periods and suppression durations. During this process, mass was transferred into the air and the water.
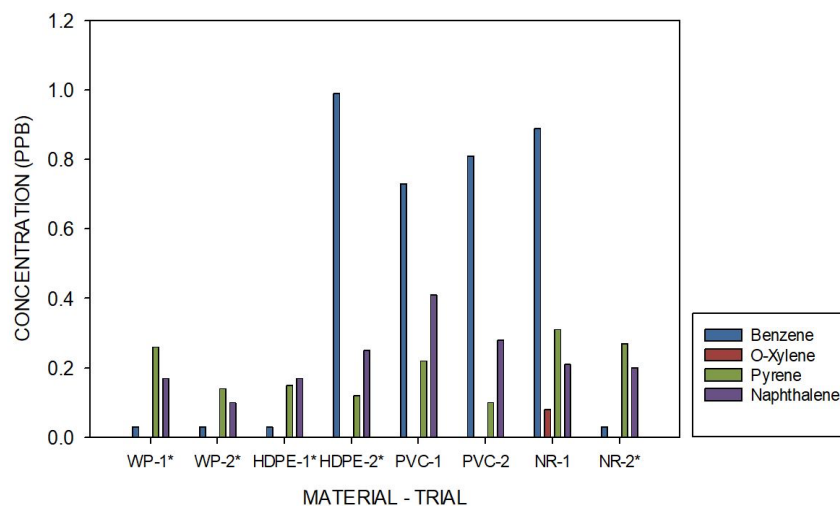

Figure i. Concentration of contaminants.

* indicates samples were reconstituted and may have lower concentrations of volatiles.

As shown in Figure i, GC-MS analysis detected benzene, pyrene, and naphthalene in all of the samples, and o-xylene was found in one sample (Neoprene Rubber 1). However, ethylbenzene and anthracene were not detected in any of the samples. Evaporation occurred in five of the samples before analysis and likely removed some of the volatile contaminants previously present in the sample. Other peaks identified in the GC-MS results were consistent with literature as well, most notably the presence of n-Hexane in all samples. Further additional contaminants not previously identified in the literature—such as 2-methoxy-4-propylphenol, cyclohexane and amylene hydrate—were present in at least four samples.

Conclusions and Recommendations

The goal of this project was to conduct research in the field of contaminant mobilization in water due to fire events. A few recommendations to improve the design and continuation of the project include:

- Improve current design of combustion/suppression method, including testing more materials.
- Improve analytical testing methods to identify and quantify a larger range of contaminants.

List of Figures

`

List of Tables

Table of Contents

`

1.0 Introduction

The destruction and devastation caused by wildfires and structure fire events they cause have been highly publicized in the last decade, most significantly in the Western United States and Australia. These events are predicted to increase in the coming decades with the onset of more extreme temperatures correlated to climate change (Abatzoglou et al., 2016). While it is easy to get caught up in the surface level damages caused by these incidents, there are potentially unforeseen challenges linked to the thermal degradation of various materials involved in these occurrences, such as water sources and the surrounding environment. Of these unforeseen challenges, pollution poses a significant obstacle to managing human and environmental health and safety—as run-off water percolates into the surrounding soil, enters waterways, and/or contacts the water supply system (Martin et al., 2016). Chemical pollution caused by fire events can result in long-lasting and detrimental effects to the health of humans and the local environment (Zhang et al., 2010). Through the careful identification of these pollutants, appropriate mitigation strategies to block potential distribution pathways and toxic effects can be designed and employed (Martin et al., 2016).

The goal of this project is to provide further insight into the contribution of thermal degradation of plastics and household materials to environmental and water contamination, as a means to promote community and environmental resilience. To reach this goal, the following four objectives have been identified:

1. Identify common materials involved in fire events that could potentially contribute to environmental degradation through contaminant mobilization, and the materials' behavior during combustion.
2. Develop a standardized burn method that is scientifically based, safe, repeatable, and that maximizes the amount of contaminants during suppression.
3. Develop an effective method to identify expected aqueous contaminants.
4. Quantify the contaminant concentration released into water during fire events.

Through these objectives, the results of this study will provide further analysis into the chemical contaminants produced—and potentially mobilized—in select building and

1

`

infrastructure materials following heat exposure, thermal degradation, and suppression by water application.

2.0 Background

The following section introduces the background to suppression-initiated mobilization of combustion-based contaminants, the fundamentals of mass transfer in fire-water mobilization, contaminant mobilization in thermally degraded piping infrastructure, and other pathways of the mobilization of the products of combustion. These sections will establish the necessity to further identify what building components and products release and potentially mobilize hazardous contaminants during combustion and suppression of residential fire events, to improve both short-term and long-term community and environmental resilience.

2.1 Evolving Infrastructure and Suppression Initiated Mobilization

Due to the recent increase in fires and media attention given to these events, thorough research is a necessity for resiliency. In 2020, approximately 52,000 fires destroyed more than 17,000 structures (Whelton et al., 2022). During fire events, large quantities of water are used as a means of suppression. While this suppression method is effective, these large quantities of water can potentially produce a significant amount of run-off and contaminant mobilization into nearby water sources.

Mobilization impacts can be characterized by both short-term and long-term effects. While the short-term impacts are readily apparent within a community, long-term impacts may be less apparent. Harmful impacts are expected to increase as new building products made from synthetic plastics and polymers continue to trend upward in the construction community. In general, these materials tend to release more harmful and carcinogenic agents when burned, compared to their natural predecessors (Fischer & Varma, 2016).

Building fires account for only 25% of the total fires nationwide; however, they are considered the most dangerous to water pollution (Proctor et al., 2021). These fires, whether they are human-made or incidental building fires, can lead to harmful toxins being released into local water streams by mobilization through natural conditions. When a building burns, a fire

suppression method is used and can lead to these chemicals traveling into local water systems and contaminate a community's water resources (Whelton et al., 2022). Additionally, once a fire is started in a building, sprinkler systems will activate to attempt to suppress the fire. If the fire is too large, firefighters will use a large quantity of water to suppress the spread of the fire, which leads to a significant amount of run-off. This could potentially drain into local waterways and/or aquifers, risking contamination. Surrounding ecosystems and watershed communities heavily rely on their water resources. If these resources become contaminated, recovery to a clean water source could take months to years or longer.

This is exemplified in the 1986 case study of the Sandoz chemical warehouse, located in Basel Switzerland. As efforts proved unsuccessful controlling this fire with foam, firefighters turned to the Rhines river as a source of water for suppression. Over several hours applying approximately 105 gallons/second (400 L/s) of water, firefighters were able to successfully extinguish the fire. The water used to extinguish the Sandoz chemical warehouse fire was ultimately recycled back into the Rhines river as a result of stormwater drainage systems. While there was a small quantity of fire-water runoff in comparison to the amount of water used for suppression, the toxins within the burning building and the synthetic materials contained therein (i.e. synthetic fabrics, rubber, and plastics) created long-term and devastating ecological impacts.

2.2 Mass Transfer of Chemical Contaminants in Fire Events

During fire events, chemical contaminants are produced due to chemical reactions converting household materials into hazardous compounds. These chemicals may be mobilized due to various mass-transfer phenomena. A multitude of materials have the ability to burn and fuel a fire. However, these materials typically do not burn completely (Speight, 2020). Complete combustion occurs when the fuel is stoichiometrically combusted into mainly water and carbon dioxide. In complete combustion, other elemental gas and oxides can also be produced, depending on the chemical composition of the fuel. When incomplete combustion occurs, ash, soot, smoke, and other hazardous organic and inorganic compounds can be produced. Typical combustion products include heavy metals, particulate matter, polycyclic aromatic hydrocarbons (PAHs), environmentally persistent free radicals, dioxins, etc. (Lomnicki et al., 2014). These materials are hazardous and can contaminate water resources.

`

Contaminants produced through combustion can enter water sources due to mass transfer. The contaminants from fire events are typically released as gas or solid particulates (Lomnicki et al., 2014). But as liquid water is introduced during fire suppression, these gas or particulate contaminants can dissolve into the water and be carried to other locations. Large quantities of water are used to suppress structure fires each year and this water is left to drain into sewer systems, the soil, or nearby water bodies. Once this contaminated water enters drinking water sources, the contamination will diffuse through the system.

2.3 Mobilized Contaminants in Drinking Water Infrastructure

In the aftermath of the most recent wildfire events in California—the Tubbs Fire (2017), Camp Fire (2018), and CZU Lightning Complex Fire (2020)—contamination of volatile organic contaminant (VOC) was detected in multiple drinking water systems (Proctor et al., 2020). One of the most hazardous of these VOCs detected was benzene—a known carcinogen (Kizer, 2020). Benzene was discovered in damaged drinking water systems at concentrations as high as 40,000 $\mu g\ L^{-1}$ immediately after the fire, and in concentrations greater than 2217 $\mu g\ L^{-1}$ two months after the containment of the fires (Proctor et al., 2020). These levels exceed the federal and California state long-term drinking water exposure limits by a factor of 200 to 40,000, as well as the California short-term exposure limit of 26 $\mu g\ L^{-1}$ (California Water Boards, 2018), and the 200 $\mu g\ L^{-1}$ limit of the United States Environmental Protection Agency (EPA) (U.S. Environmental Protection Agency, 2018). As for the time frame required for contaminant removal, collected site samples revealed benzene concentrations of 530 $\mu g\ L^{-1}$ six months following containment of the Camp Fire, and in the end, over one year was required to completely alleviate the chemical contamination in surrounding water distribution systems (Spearing, 2020).

Wildfires have also prompted the identification of other VOCs in drinking water systems and waterways. These VOCs include, but are not limited to, dichloromethane, naphthalene, styrene, tert-butyl alcohol, toluene, and vinyl chloride (Whelton et al., 2019). Furthermore, semivolatile organic compounds (SVOC) also pose a contamination risk, being detected in distribution systems following the Tubbs Fire and in the ash of the Camp Fire (Isaacson, 2020). Specifically, what other VOCs were possibly produced in these fires, in addition to

dichloromethane and naphthalene, is unknown, because drinking water testing for these contaminants was limited over the course of this study.

It can be hypothesized from case studies that the underlying cause of contamination is the result of the thermal degradation of plastic materials present in water systems damaged by the fire and other household materials involved in fire events. Additionally, given the research on long-term contamination of water systems post-wildfire, it can be hypothesized that residential fires will have a similar or greater effect on local water systems due to the increasing application of plastics and other materials in everyday household items and closer proximity to built and environmental water systems.

2.4 Growing trends in Piping Infrastructure

Because of their adaptability and low cost, plastic and rubber piping are increasingly being used for water distribution, purification systems, and building plumbing in the United States and Canada (Folkman, 2018). Polyvinyl chloride (PVC) and high-density polyethylene (HDPE) are the two most common materials used in water distribution pipes, and neoprene rubber tubing is the most commonly used in basic household water line transfer and purification systems (Rockaway, 2007). Figure 1 provides a breakdown of the most common PVC applications worldwide in 2013 with pipes/fitting taking a majority at 43% (Yu et al., 2016).
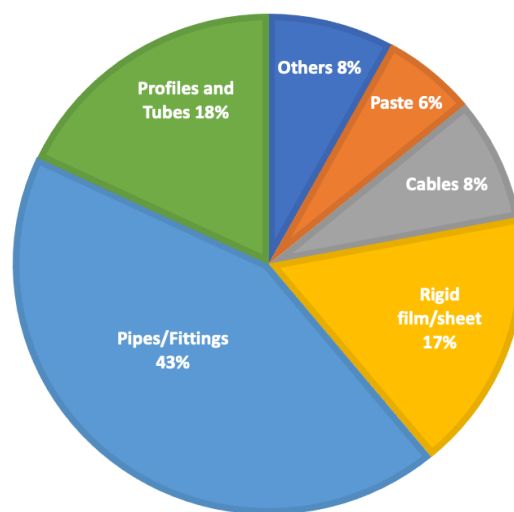
Figure 1. Worldwide PVC application in 2013, totaling 38.5 million tons (Yu, et al., 2016).

`

Approximately 85% of the water mains and service lines impacted by the heat of the Tubbs Fire were PVC (Whelton et al., 2019). Within the Paradise Irrigation District, Paradise, CA, as many as 10,480 service lines contain a variety of crosslinked plastics, consisting primarily of PVC and HDPE (Paradise Irrigation District, 2019). There is also a large amount of PVC and HDPE piping in building water conveyance systems. Service lines and building piping are often 5 to 10 times the length of the underground piping in water distribution systems (Loganathan, 2005). It should also be noted that private drinking water wells are also known to contain PVC and HDPE pipes, and service lines are often lined with neoprene rubber tubing. Because of this, California and Oregon state agencies advised private well owners to test for VOCs and SVOCs following the containment of the Camp Fire and CZU Lightning Complex Fire (County of Santa Cruz, 2020).

In spite of the worrying release of VOCs into the air as a direct result of burning structures and the understanding that the large volume of water used in firefighting activities is contaminated through contact with fire debris or smoke, the identity of the hazardous contaminants in water and their potential to negatively impact water distribution system has been the topic of few studies (Isaacson, 2020). Current research into the identification of contaminants found in the air following the thermal degradation of PVC, HPDE, and neoprene rubber include benzene, ethylbenzene, toluene, xylenes, chlorobenzene, and naphthalene, among other hazardous chemicals (Aracil et al., 2005, Ueno et al., 2010, & Lam et al., 2020). As stated previously, a majority of these compounds were detected in the drinking water following containment of the Tubbs, Camp Fires, and CZU Lightning Complex Fire.

However, in a recent study conducted by researchers at Middle Tennessee State University, "Releases of Fire-Derived Contaminants from Polymer Pipes Made of Polyvinyl Chloride," a series of PVC pipes were set aflame with a propane torch and then submerged in water for 7 days, which produced vinyl chloride and chlorobenzene—two contaminants identified in drinking water samples from the Tubbs Fire and Camp Fire—but not benzene (Chong et al., 2019). These results further emphasize the need to investigate these plastics, common piping materials, and other abundant household materials that undergo thermal degradation during wildfires and house fire events.

2.5 Exploring Further Pathways of Mobilization

Along with the production of plastics—growing worldwide at an estimated 5% increase each year; reaching over 150 million tons of plastic produced per year—there has been an increase of disposable plastics (Valavanidis, 2007). Primary examples of everyday disposable plastic waste include the following: high and low density polyethylene (HDPE, LDPE) used in shopping bags, food wrap, and films; polyvinyl chloride (PVC) used for bottles, packaging, and containers; polyethylene terephthalate (PET) used in beverage bottles and similar containers; polystyrene (PS), the spongy white material used in food containers, hot beverage cups, and insulating materials; and polypropylene (PP) used for yogurt containers, diapers, wrapping films, butter tubs, etc. Each of these plastics is typically discarded after use as household waste. A high proportion of these plastics are disposed of alongside municipal waste in landfills. In recent decades, under the pressure of high volumes of plastic and other packaging waste, Western Europe, Greece, India, and Japan have begun to consider or implement solid waste incineration facilities. Burning these materials in incinerators would drastically reduce the volume of waste and produce electricity simultaneously, in some cases (Simoneit et al., 2005).

There are already several environmental concerns regarding potential toxic effects associated with the disposal of plastics in landfills, including bioaccumulation in aquatic organisms and the release of hazardous substances during disposal in municipal waste sites. These conscience are expected with the addition of combustion, as burned plastics can generate VOCs, smoke (particulate matter), particulate-bound heavy metals, PAHs, polychlorinated dibenzofurans (PCDFs), and dioxins. The fumes and soot produced through plastic combustion, which can severely increase in instances of plastic combustion in building fires, have the potential to mobilize into the air, ground, and nearby water sources (Shemwell et al., 2000).

A major concern in terms of contaminant conveyance for open landfill incineration, wildfire, and building fire events is precipitation, especially the phenomena typically referred to as the first flush. In an analysis of several studies conducted by the University of California Los Angeles Department of Civil and Environmental Engineering, it was found that most of the contaminants had approximately 50-80% of their total mass mobilized during the first 50% of rainfall volume (Stenstrom, 2005). Moreover, as transportation infrastructure continues to grow

7

across the United States and the globe, urban stormwater runoff and first flush will continue to persist as one of the leading causes of contamination in receiving water bodies (Lee et al., 2001). These urban pathways work in conjunction with the first flush effect to mobilize a large variety of contaminants from high density settlements to forests, rivers, and other natural environments, where they infiltrate water supplies and pollute natural ecosystems.

The environmental risk associated with these concerns becomes more evident when considering a study conducted at the University of Athens (Valavanidis, 2007). In the study polymeric materials were burned in simulated landfill incineration conditions. The polymeric materials burned included PS, PVC, LDPE, HDPE, PP, and PET. These polymeric materials were selected based on common plastics in landfills and common household products (Valavanidis, 2007).

The resulting soot and ash were analyzed following experimental simulation through electron paramagnetic resonance. All plastics burned had similar free radicals found in airborne particulate matter in urban and industrial areas with high levels of atmospheric pollution. Solid ash was analyzed through Inductively Coupled Plasma Emission Spectrometry, and all plastics revealed high amounts of lithophilic metals (sodium, cadmium, silicon, magnesium, and iron), with PVC recorded the most heavy metals (lead, nickel, chromium, aluminum, and copper). Soot and ash also revealed twelve PAHs: naphthalene, acenaphthene, fluorene, phenanthrene, anthracene, chrysene, and six other PAHs with known carcinogenic potential: benzo[a]anthracene, benzo[k]fluoranthene, benzo[b]fluoranthene, benzo[a]pyrene, dibenzo[a,h]anthracene, and indenol(I,2,3-c,d)pyrene, through analysis involving the application of Reversed-Phase High-Performance Liquid Chromatography (Valavanidis, 2007).

2.6 Community and Environmental Risk

Roughly 80% of the U.S's drinking water originates from forested land, and more than 3,400 communities located near forested lands rely on the area's watershed (Murphy et al., 2015). Understanding both the long-term and short-term effects of the hazards produced and mobilized during fire events is key to providing communities with resiliency tools to form quicker and less costly pathways to environmental recovery. In 2019 alone, community water providers in Colorado spent more than $26 million on water-quality treatment and

`

debris/sediment removal, following two devastating wildfire events (Resources, 2019). While understanding conveyance systems for contaminant mobilization is more confined to the geography, climate, topography, and other factors of communities, the origins of contaminants are typically traceable. Therefore, understanding what building components or products release which hazardous contaminants as a result of thermal exposure or combustion, and how these hazards impact the water supply—as well as air and soil—is a universal step toward environmental and community relief.

3.0 Methodology

The goal of this project was to provide further insight into the contribution of thermally degraded plastics and other household materials to environmental and drinking water contamination. The following four objectives were used to accomplish this goal.

1. Identify common materials involved in fire events that could potentially contribute to environmental degradation through contaminant mobilization, and determine the nature of these materials during combustion.
2. Develop a standardized burn method that is scientifically based, safe, repeatable, and will maximize the amount of contaminants during suppression.
3. Develop an effective method to identify expected aqueous contaminants.
4. Quantify contaminant concentration in water released during fire events.

Sections 3.1–3.6 summarize the team's combustion and suppression methods and experimental procedures, while sections 3.7–3.14 summarize methods for contaminant analysis and identification. In essence, each section describes the methods implemented by the team to meet the goal and objectives.

3.1 Pre-Crib Construction

When designing the experimental procedure, materials were selected based on the ease of access and occurrence within the built environment. The four materials selected were HDPE, chemical resistant PVC, neoprene rubber, and white pine wood. HDPE and PVC materials were selected due to their frequent implementation in buried water mains, buried service lines, and in building plumbing systems (Busse, 2005). Neoprene rubber has applications in common

household electronics, basic water transfer systems, water purification systems, automobile parts, and specific clothing items (Rockaway, 2007). Pinewood and plywood (which primarily consists of pinewood) is used in furniture, kitchens, and structures (including exteriors, framework, and flooring). Over the last two decades, 99.4 percent of the total 192,000 cubic meters of pinewood and plywood manufactured in Australia was used for these purposes (Lam, 2020). Additionally, the U.S. plywood market reached a value of $8.5 million in 2020 (Chudy et al., 2020). Ultimately, these four selected materials allowed for an accurate simulation of a structural fire, to provide analysis of the potential contaminants released post-fire into local water sources.

3.2 Crib Construction

A crib typically consists of uniformly cut blocks of wood or "sticks." The sticks are equally spaced in a plane, typically called layers; the layers are stacked in an alternating pattern as seen in Figure 2. For the purposes of this procedure, The use of cribs was selected due to their high repeatability in burning rate, depending on stick thicknesses and arrangements, and their radiative heat qualities. Stick thicknesses, spacing, and number of layers were selected empirically and proportionally from previously successful crib suppression and burning rate studies (Kung and Hill, 1975 & McAllister and Finney, 2015).
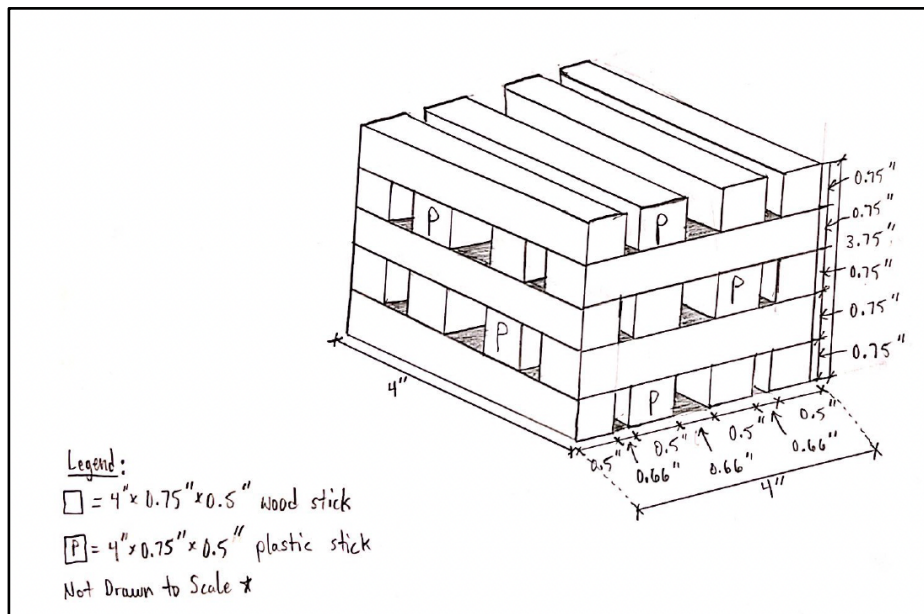
Figure 2. Wood and polymeric crib design with dimensions.

`

As shown in Figure 2, each crib was constructed with sticks that are 4 inches long by ½ inches wide by ¾ inches tall. Sticks were spaced ⅔ inches apart (for a total of 4 sticks per layer) to encourage a sufficient radiative heat exchange between fuel elements and a steady burning rate under 1 g/s. After the addition of 5 layers each crib yielded a height of 3.75 inches and the length and width of 4 inches.

As a significant amount of thermal radiation would be required for the combustion of neoprene rubber, PVC, and HDPE, only 5 sticks of the testing material were included in each crip (marked by P in Figure 2). A consistent ratio of 25 percent testing material to 75 percent pinewood was used in each crib, including 2 completely pinewood cribs.

To fully ignite each stick within the crib and achieve a steady-state burning rate across the surface area of all four crib compositions, a heptane pool fire was selected as the optimal method for combustion, as this method provides a constant heat flux (W/m^2).

3.3 Steady-State Curve Generation

To encourage contaminant mobilization during suppression, it is important to achieve steady state before suppression. To determine when this steady state period was, a preliminary burn was done for each crib. These burns were not suppressed, and burned until extinction on a load cell while mass data was continuously collectly.

After these preliminary burns were completed, the mass data was graphed against time, and then used to create four mass-loss-rate versus time curves. The flat regions of the mass-loss-rate vs. time curves corresponded to the steady state period for each crib, indicating the duration and when it began and concluded. An image of each of the cribs at steady-state burning can be observed in Figure 3.

In addition to steady-state curves generated without suppression, burns with suppression were also completed. During these trials, steady-state periods coincided with the steady-state periods reached during preliminary trials without suppression, aiding in experimental consistency and predictability. Cribs suppression stopped once a new steady state period was clearly observable within the real time load cell data computer program.
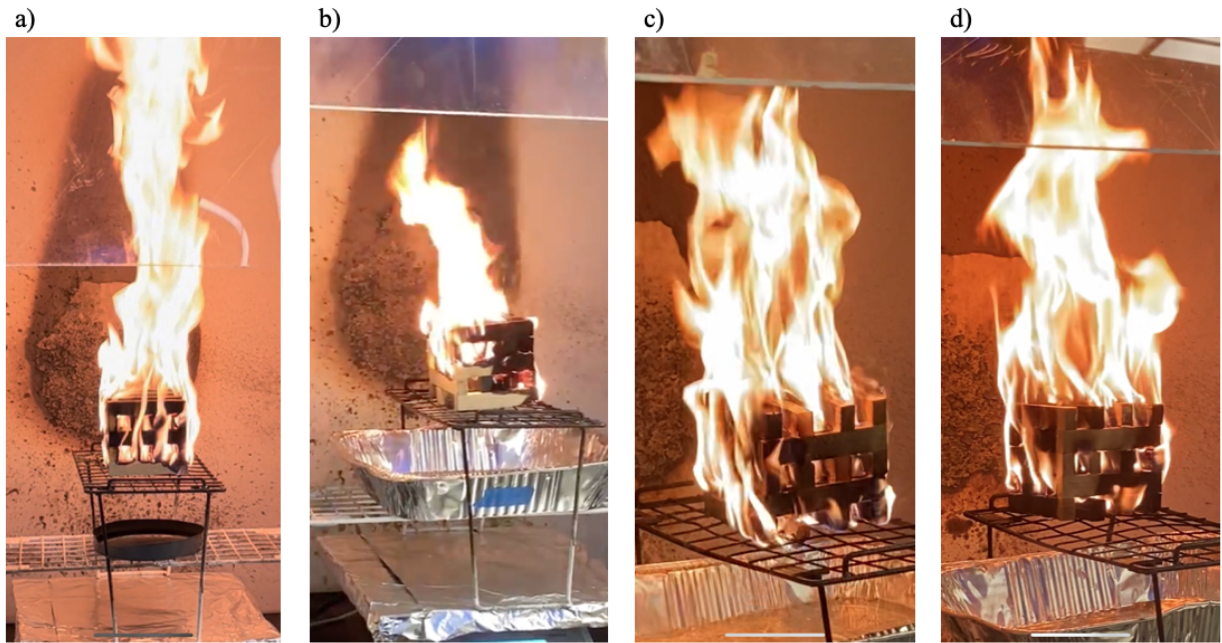
Figure 3. Pinewood (a), PVC (b), HDPE (c), neoprene rubber (d) during periods of steady state burning.

3.4 Suppression System Construction

To suppress the cribs in a consistent manner, a suppression system was designed to allow for adjustment to the flow rate of the water, as well as even distribution of water across each crib.

To accomplish this six 0.0160 inch holes were drilled into three sections of ¼ inch stainless steel threaded pipe. The sizing of these holes allowed for water to be pushed through, instead of flowing through. This aided in even distribution of water through each hole and across the crib during combustion. Water was moved from a reservoir through the suppression system using a peristaltic pump.

To further encourage even water distribution, the pipes were primed with water before ignition was propagated. Additionally, priming the pipes introduced added thermal mass inside the pipes that absorbed the heat of the flame, preventing any heat damage to the pipes.

Empirical evidence suggests a correlation between heat release rate to the flow rate of water needed for suppression (Magee and Reitz, 1975). An estimated flow rate of 6-600 ml/min

of water was needed to suppress and not extinguish each crib, based on the calculated heat release rate of a 4x4x3.75 inch pinewood crib.

3.5 Combustion and Suppression Experimental Setup

A consistent experimental setup and combustion procedure was maintained for each crib burn throughout the study. This setup is shown in Figure 4.
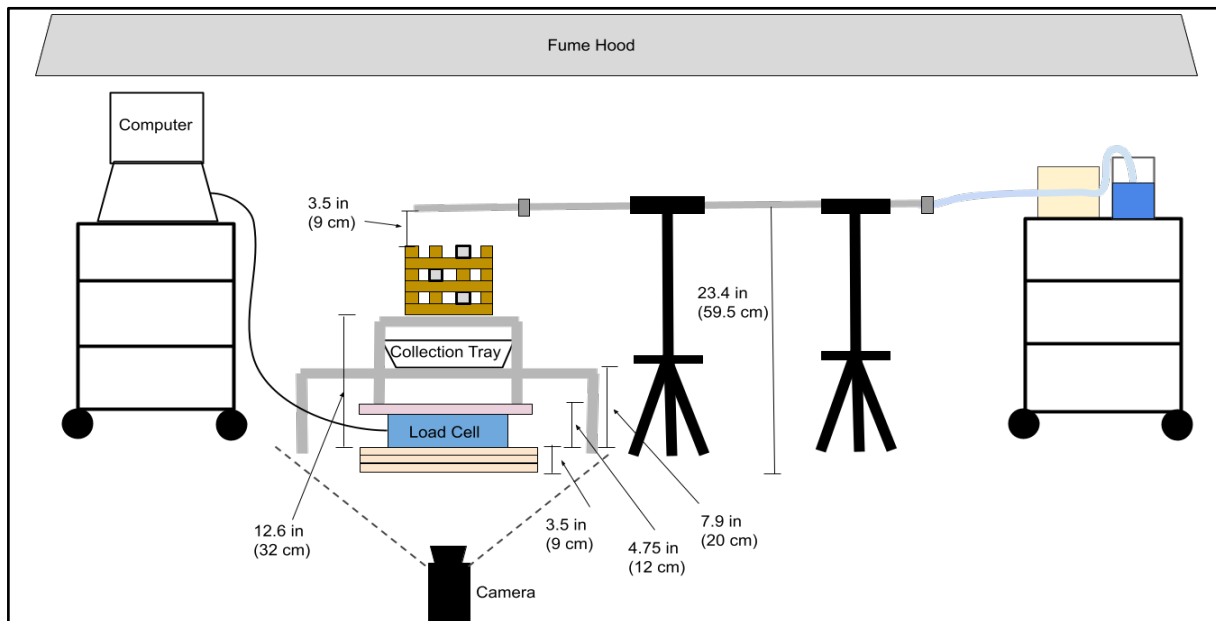
Figure 4. Combustion and suppression experimental setup.

The load cell (6.5 kg capacity and 0.01 g sensitivity) was placed on top of sheetrock stacked to 3.5 inches above the ground, to protect the floor and elevate the crib so that it is closer to the suppression system. The mass of each crib as it was burned was collected over 25 second intervals, and stored and processed using the program LabView. On top of the load cell was a 13 by 13 inch foam board that was wrapped in aluminum foil to prevent possible ignition. The foam board was used to increase the loading surface area. Two wire racks were used so that the collected water did not interfere with the mass measurements of the burning crib. The larger of the two wire racks (18 inches long by 7 inches wide) was placed over the load cell, touching the floor. This rack held an aluminum collection tray and a heptane pool fire. The second wire rack

(13 inches long by 7 inches wide) was placed on the foam board and extended over the larger wire rack, with the longer side lining up with the short side of the larger wire rack.

The water suppression system was above and extended to the right of the data collection setup. A 5000 mL reservoir of distilled water was connected to a Masterflex L/S standard digital drive with remote capabilities, 16–100 rpm, 115V peristaltic pump with Masterflex L/S 17 Precision Pump on top of a wheeled cart. The outlet of the pump was hooked up to the rest of the suppression system using Masterflex L/S 17 Precision Pump Tygon Tubing. This tubing was connected to a ¼ in diameter, three-foot-long metal pipe using a barbed adapter. This metal pipe was 23.5 inches above the ground and was supported using two tripods. The metal pipe was attached with a four-way fitting. The three other connections were fitted with a ¼ inch diameter intermediate thread attachments. Elbow connections were attached to the two side connections. A 1 foot long, ¼ inch diameter pipe with six 0.0160 inch holes drilled in it was attached to each of the thread attachments, to form the basis of the three-pronged suppression system (Figure 5).
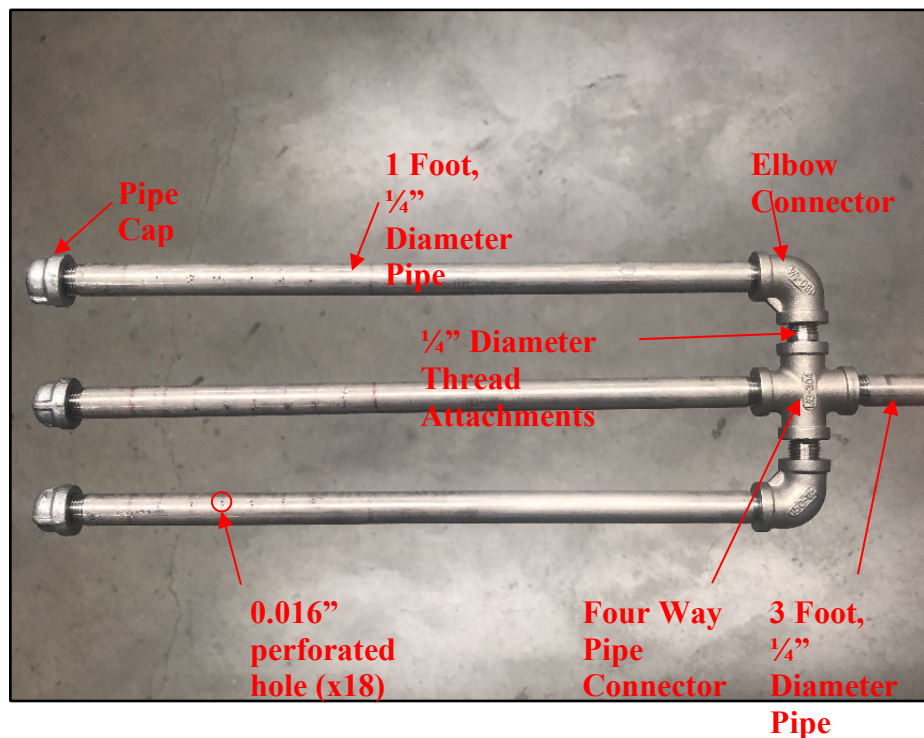
Figure 5. Three-pronged suppression system.

`

3.6 Combustion and Suppression Experimental Procedure

The suppression system was primed by activating the system at a flow rate of 150 mL/min and, after being primed, the suppression system was switched off. Before placing the crib on top of the smaller wire rack, the load cell was zeroed. A 5-inch diameter stainless-steel pan filled with approximately 10 mL of heptane was placed on top of the larger wire rack directly under the crib. Before each burn this pan was ignited with a propane torch. Upon ignition of the heptane, LabView was initiated on the computer to record mass loss vs. time data. After the heptane fire reached extinction, the empty 5-inch diameter stainless-steel pan was removed, and an aluminum collection tray was placed directly underneath the crib. Once steady state was reached for each burn, the peristaltic pump was reactivated and distilled water was pumped through the pipes for 100 seconds (the mean steady-state-duration time for each crib composition) or until a new steady-state burning period was reached. All water collected in the aluminum collection tray was transferred to a 125 mL glass container via pipette. Coarse grain filters were applied over the container during water collection. This prevented the transfer of any excess materials into analysis samples.

3.7 Selection of Contaminants

The contaminants analyzed were chosen based on two criteria: their position of concern in water resource contamination, and their presence in materials commonly found in residential settings. A preliminary list of contaminants to analyze was developed based on the primary national water contaminant list (EPA, 2018) and chemicals found in water supplies after wildfires (Valavanidis et al. 2008, Smith et al. 2011, Fent et al. 2018). This list was then narrowed down based on previous studies on contaminants released from materials during burns (Chong et al. 2019, Lam 2020), and all contaminants' ability to be analyzed with Gas Chromatography-Mass Spectroscopy (GC-MS). From this list (Appendix A), the following chemicals were chosen as a group of indicator chemicals: benzene, ethylbenzene, o-xylene, pyrene, naphthalene, and anthracene. These contaminants were expected to appear in the collected samples of water.

`

3.8 Normalization of Samples

Every water sample was stored at 4 ºC after collection and before filtering. The samples were stirred vigorously on a stir plate to ensure a homogeneous mixture, and any volume of sample collected over 50 ml was stored to be discarded later.

3.9 Initial Filtration

To prevent clogging of the solid phase extraction (SPE) cartridge and damage to the GC-MS during analysis of the samples, the water used to extinguish the residential fire simulations was filtered via vacuum filtration to remove insoluble contaminants and debris. Each 50 ml sample was stirred and allowed to settle for 2 minutes, to avoid clogging the filter paper and to allow for more effective filtration. Each sample was then slowly poured into a funnel of a vacuum filter fitted with a 90 cm diameter glass fiber filter membrane with a 0.45 μm pore size (Hawach Scientific MLGF90045). After the entire 50 mL sample was filtered, the sample was then run through SPE.

3.10 Solid Phase Extraction (SPE) as Pre-Processing of Liquid Sample

The SPE cartridges (Supelclean™ ENVI™-18 SPE Tube, bed wt. 500mg, volume 3 mL) were conditioned with 2 mL of methanol, followed by 2 mL of reagent grade water to activate packing before the extraction. After the completion of conditioning, the samples were pumped at a flow rate of approximately 1 mL per minute through the cartridges. After each entire sample passed through its cartridge, 4 mL of reagent grade methylene chloride was drawn through each cartridge to elute the analytes. These processed samples were collected and stored at 4ºC, then analyzed using the GC-MS.

3.11 Reconstitution of Evaporated Samples

After the 4 mL samples were prepared with the SPE, they were stored at 4ºC. Due to an inefficient seal of our test tubes and the volatile property of methylene chloride, portions of most of the samples evaporated. Only a small amount of these samples remained and were likely to be missing some volatile contaminants. Thus some of the contaminants of interest could have evaporated out with the solvent. However, not all of the contaminants are very volatile and

`

visible residues were observed on the sides of the test tubes that those samples were stored in. This called for a reconstitution of the samples.

To reconstitute each sample that had evaporated, enough methylene chloride was added to the test tube so that the entire volume of the sample was approximately 4 mL. 4 mL of methylene chloride was measured using an auto pipette and added into a clean test tube. This "4 mL test tube" was used to visually measure the volume of the contents of the sample test tubes. It was covered and placed in a test tube rack, standing upright. Then each sample test tube was individually placed next to it and reagent grade methylene chloride was slowly added to the sample test tube, using a pipette, until the sample test tube's meniscus lined up with the 4 mL test tube. After each sample was reconstituted, it was stored, covered, at 4ºC for two hours. This allowed for the contaminants to redissolve into the methylene chloride; the samples were then poured into airtight sample bottles for proper storage at 4ºC.

3.12 Standard Preparation

Two sets of standards were purchased from MilliporeSigma covering all major contaminants considered. The two sets of standards—Supelco EPA 625 Semivolatile Calibration Mix and Supelco EPA 502/524 Volatiles Organic Calibration Mix (without gasses)—were purchased. The concentration of each contaminant for EPA 625 was 1000 μg/mL and for EPA 502/524 was 2000 μg/mL. The full list of components of each standard is listed in Appendix B.

A 4-step serial dilution with reagent grade methylene chloride was performed to create several samples of each standard at a known concentration ranging from 100 ppb to 0.1 ppb (Table 1) (Anderson, 2019).

`

Table 1. Serial dilution.

	EPA 625	**EPA 502/524**
Initial Concentration	1,000 ppb	2,000 ppb
Step 1	100 ppb	100 ppb
Step 2	10 ppb	10 ppb
Step 3	1 ppb	1 ppb
Step 4	0.1 ppb	0.1 ppb

In all the steps in the serial dilution for EPA 625 and steps 2-4 of EPA 502/524, 0.5 ml of the previous solution was added to a 5 ml volumetric flask using a volumetric pipet, and the rest of the flask was filled with methylene chloride. For the first step of EPA 502/524, 0.25 ml of the standard was used. Vials and pipettes were cleaned according to the cleaning procedures in section 3.14.

Standard curves were created using the 10, 1, and 0.1 ppb diluted standards, run through the GC-MS. These standard curves were used to determine the concentration of each contaminate present in the samples.

3.13 Gas Chromatography-Mass Spectrometry Analysis

GC-MS was used to measure the organic contaminants in each sample and the standards. Before running, each sample was filtered using a 5 mL syringe with a 0.45 μm filter attached. The samples and standards were then placed into 1.5 mL GC vials. An Agilent Technologies (Santa Clara, CA) 7890B system with a 5977B MSD was used to complete the analysis. The equipped column was an HP-5ms ultra inert 30m x 250 μm x 0.25 μm. The GC oven was initially set to 40°C for 4 minutes (Anderson, 2019). The oven temperature was then increased to 290°C at a rate of 9°C/min and then held at 290°C for 6 minutes. The sequencing time was set to 44 minutes for each vial and 2.0 μL samples were injected in spiless injector mode. The thermal aux transfer line to MS was set to 200°C. Helium gas was used as a carrier gas at flow rate of 1 mL/min, an inlet temperature of 500°C, a mass scanning range from 50 to 500, and a pressure of 7.8 psi.

`

An online chromatogram modeler, Pro EZGC Chromatogram Modeler
(https://www.restek.com/en/technical-literature-library/brands/EZGC-online-tools/), was used to
predict the expected retention time for the contaminants that were analyzed. It was used to
analyze the extent of overlapping peaks that were expected under these GC-MS conditions. A
full list of the expected outputs is in Appendix C. These simulations allowed for more efficient
analysis of the samples and reduced the need for repetitive recalibration.

3.14 Cleaning Procedure

To reduce cross contamination, all glassware was cleaned with the following process,
based on the procedure used by Anderson (2019). First, all glassware was rinsed thoroughly with
tap water. Then, the glassware was washed with Sparkleen 1, a lab grade detergent. Following
that, the glassware was rinsed with tap water until detergent was no longer visible. Afterwards,
the glassware was rinsed twice with purified water produced by a Barnstead Nanopure,
Barnstead RO, and Aquapure filter combined system, then left to air dry.

To remove residual organic compounds, all dried glassware was rinsed twice with
reagent grade methylene chloride. Each rinse was conducted by filling the piece of glassware to
20% of its volume and swirling with methylene chloride. To prevent excess chemical waste,
methylene chloride used once from another piece of glassware could be used to conduct the first
rinse. However, second rinses were conducted with fresh methylene chloride. Disposable
glassware such as pipettes and the vials used in the GC-MS were not cleaned using the detergent.
They were only rinsed twice with methylene chloride.

4.0 Results and Discussion

The following sections present and discuss the findings of this project. Sections 4.1–4.6
cover the results observed following steady-state trials and combustion/suppression trials for all
cribs. The steady-state and combustion/suppression trials produced largely expected results given
the composition of each crib. Sections 4.7–4.10 cover the contaminants found in each of the
water samples obtained during the suppression trails and the concentrations of five of the six
indicator chemicals.

`

4.1 Steady-State Curves
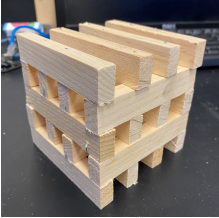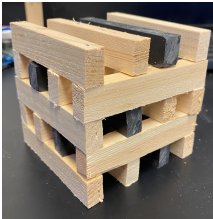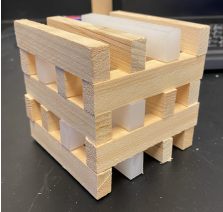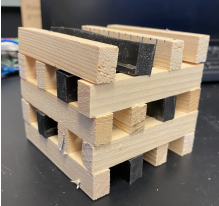
The steady-state curves are instrumental to determining when to suppress the fire, as well as how long. Preliminary burns without suppression resulted in the following steady state periods indicated by the red lines in the graphs in Figure 6 on the next page. Information gathered from the duration and rate of each steady state period was then analyzed and used to construct Table 2.

.
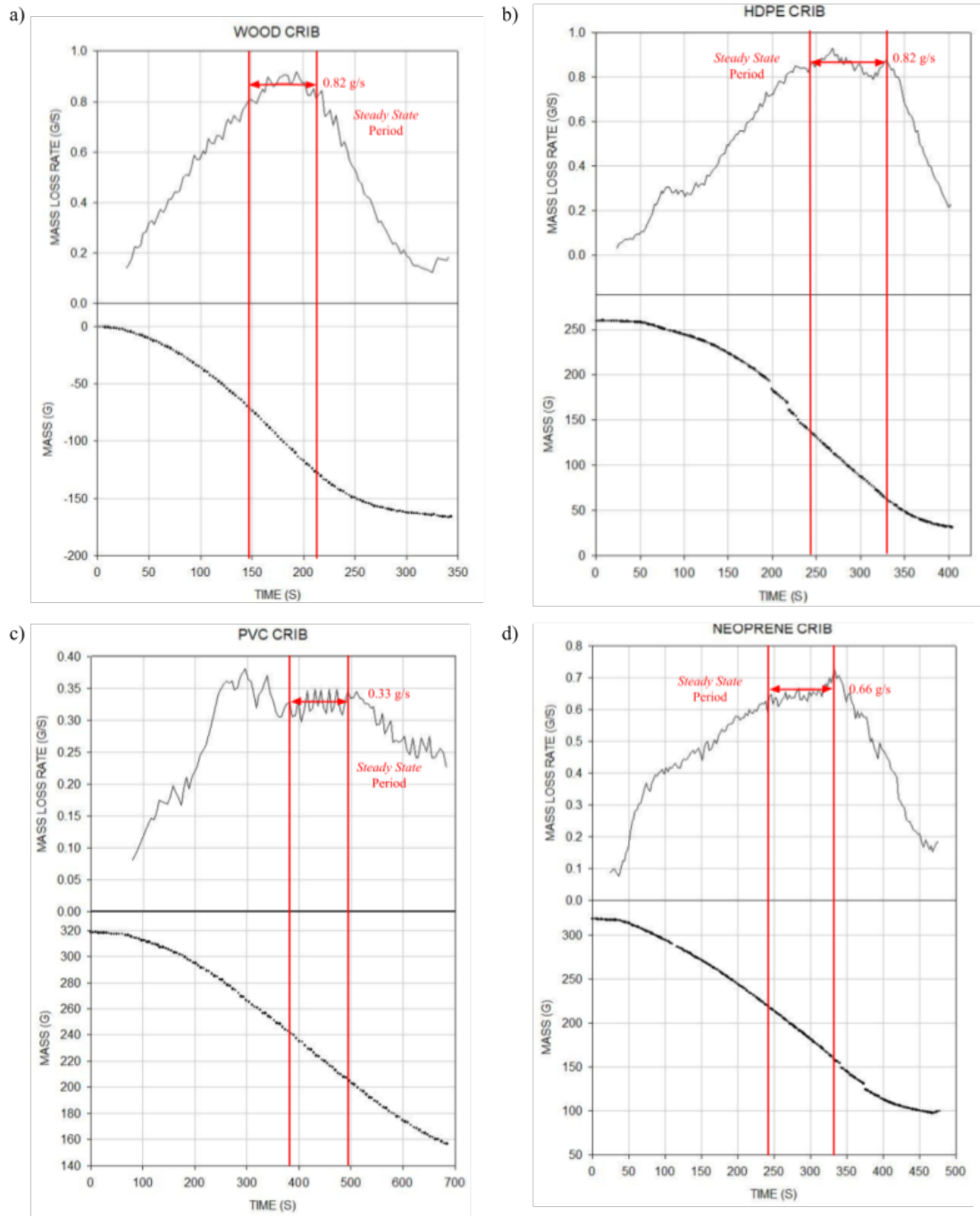
Figure 6. Mass (grams) as a function of time (seconds) and mass loss rate (grams/second) as a function time (seconds) for pine wood (a), PVC (b), HDPE (c), and neoprene rubber (d) crib compositions.

`

Table 2. Vertical gap, mass, steady state duration and average steady-state mass loss rates for pine wood (column 2), PVC (column 3), HDPE (column 4), and neoprene rubber (column 5).

Crib Composition	Vertical Gap [in]	Mass [g]	Steady State Range [s]	Steady State Duration [s]	Average SS Mass Loss Rate [g/s]	Surface Area [in²]	Porosity (Eq. #) [in]
Pine Wood							
	7.5	190.20	145-220	75	0.82	192.8	0.15
PVC							
	7.5	313.09	375-500	125	0.33	192.8	0.15
HDPE							
	7.5	249.41	230-330	100	0.82	192.8	0.15
Neoprene Rubber							
	7.5	320.28	240-340	100	0.66	192.8	0.15

`

As shown in Table 2, the average steady state duration across all cribs is 100 seconds, reaching a maximum of 125 seconds for the PVC crib and a minimum of 75 seconds for the white pine crib. The average mass loss rate during steady state across all cribs was 0.66 g/s, reaching a maximum of 0.82 g/s for wood and HDPE and a minimum of 0.33 g/s for PVC. There is a slight correlation with these mass loss rates and the mass of each crib, HDPE and white pine, the two lighter cribs, exhibited much higher mass loss rates than PVC and rubber, the heavier of the cribs.

4.2 Steady-State Curves with Suppression

Introducing suppression created significant changes in mass vs. time and mass loss rate vs. time data. To analyze these changes, Figure 7 (shown on the next page) was created, illustrating the data patterns for the mass and mass loss rate for each crib composition, per unit time, during both combustion and subsequent suppression.
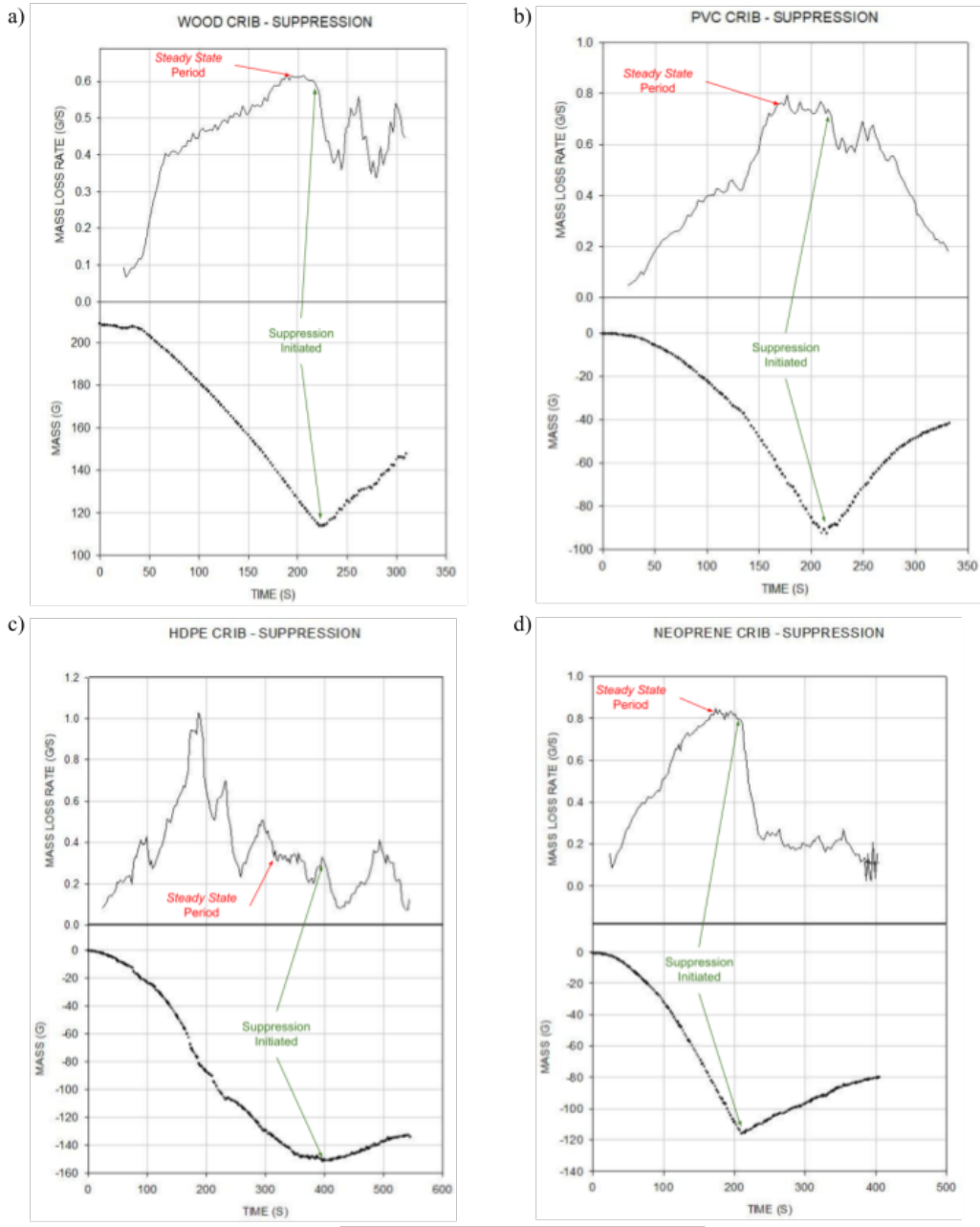
Figure 7. Mass (grams) as a function of time (seconds) and mass loss rate (grams/second) as a function of time (seconds) for each crib composition with suppression. The locations of the initial steady state period (red) and suppression (green) points are indicated. Pine wood (a), PVC (b), HDPE (c), and neoprene rubber (d) crib compositions are shown.

`

As seen in Figure 7, a new steady state duration with a new average steady-state mass loss rate is not seen following suppression (with the exception of the prominent secondary steady state period during the neoprene rubber burn). This can largely be attributed to the effect of water clinging to the surface of the wooden cribs, increasing each crib's mass over the suppression period. This can be seen in the prominent peak in the mass vs. time curves, indicating the time suppression starts. Due to this effect, we were unable to measure a new steady state during suppression. Visual cues along with referring to the steady-state data from Table 2, allowed the team to accurately observe when each crib reached steady state and therefore initiate suppression. Figure 8 is a visual timeline of each crib's combustion and suppression sequence. Table 3 (on next page) summarizes the data of Figure 7 and provides further insight into the combustion nature of each crib composition.
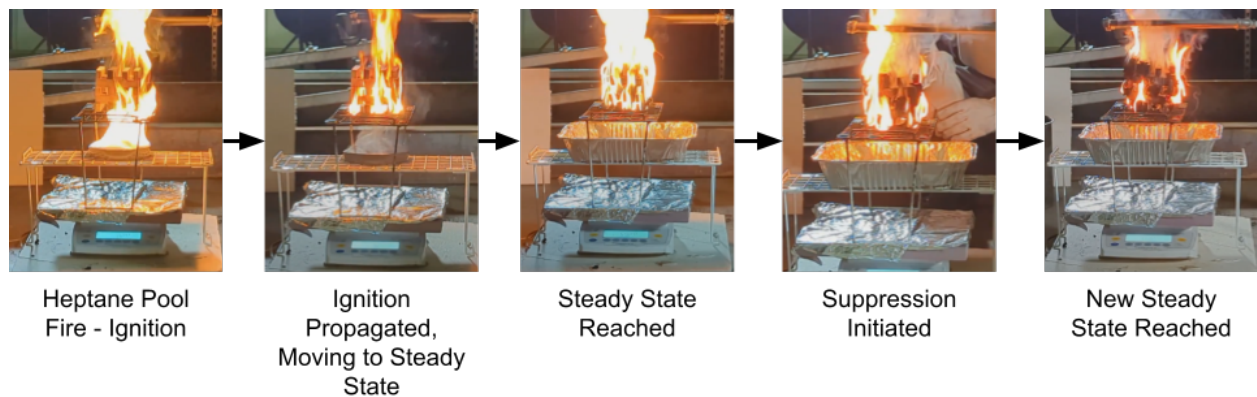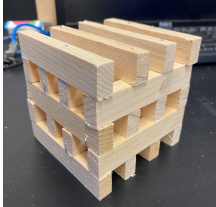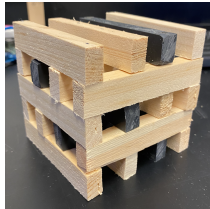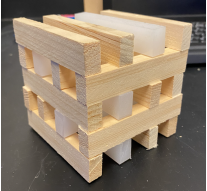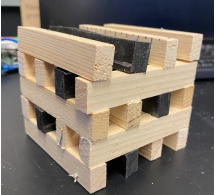
Figure 8. Burn and suppression progression of each of our materials.

`

Table 3. Secondary steady state, mass, accumulated water, suppression, and flash point data for pine wood (row 2), PVC (row 3), HDPE (row 4), and neoprene rubber (row 5).

Crib Composition	Initial Mass [g]	Final Mass [g]	Water Accumulated in crib [ml]	Secondary Steady State Range [s]	Secondary Steady State Duration [s]	Suppression Duration [s]	Flash Point [°F]
Pine Wood	210	115	35	250-315	65	90	572[1]
PVC	313.09	223	50	225-275	50	110	734
HDPE	249.41	100	13	415-550	135	150	580[2]
Neoprene Rubber	320.28	205	37	250-400	150	180	500

[1] Janse, A. M., de Jonge, H. G., Prins, W., & van Swaaij, W. P. (1998). Combustion kinetics of char obtained by flash pyrolysis of pine wood. *Industrial & engineering chemistry research*, *37*(10), 3909-3918. https://doi.org/10.1021/ie970705i

[2] Köfteci, S. (2016). Effect of HDPE based wastes on the performance of modified asphalt mixtures. Procedia engineering, 161, 1268-1274. https://doi.org/10.1016/j.proeng.2016.08.567

`

As illustrated in each of the four graphs in Figure 7, each crib burned at its initial steady state for approximately 40-60 seconds before suppression was initiated. HDPE took the longest to reach steady state for these trials, requiring 300 seconds before an initial steady state could be observed within the mass loss data—approximately 1 minute longer than the other materials.

 Once suppression was initiated, there was a period of a few seconds where the mass loss rate dropped rapidly due to the application of water. As previously mentioned, new steady state periods were difficult to distinguish and required visual cues along with referring to the steady-state data from Table 1 during the preliminary steady-state burns; however, a closer analysis of Figure 7 reveals a distinct drop in the initial steady state period over the course of 10-25 seconds for different crib compositions following suppression initiation. This drop is followed by fluctuating mass loss rates over the remaining course of Figure 7, primarily due to water attaching to each crib's surface. During this final period each crib burned at a distinctly steady and less intense rate, based on observation, until suppression was stopped. The period between the end of the drop in the initial steady state period and end of data collection marked the secondary steady state duration (except when a distinct decreasing trend in mass loss rate was observed during the suppression period, which can be observed at the 275 second mark in the PVC's mass loss data in Figure 7). This duration ranged between 90-180 seconds, and can be observed for each crib composition in the 7th column of Table 3.

Each crib burned away around 90-100 grams of material, aside from HDPE, which burned 150 grams of material. Keeping with the trend, each crib amassed a similar amount of water on their surface areas after suppression (35-50 ml), except for HDPE which accumulated only 13 ml. HDPE was the only material to melt as it burned, explaining why there was more mass lost during combustion and suppression. Also, there were actually fewer sticks remaining in the HDPE crib when suppression was initiated, resulting in less surface area for the water to bind to.

4.3 White Pine Burn Analysis

The crib consisted of only white pine wood. The crib became fully ignited within 140 seconds after ignition. The heptane pool fire successfully ignited and spread through the entirety of the crib. The flame height increased as more of the wood began to burn and the wood

developed a charred appearance. Shortly after the heptane pool fire burned out, the white pine

began to shrink and crumble. During both combustion and suppression, the crib emitted black

smoke. When suppression was initiated, particles of ash and black soot mobilized to the water in

the collection tray. This can be seen in Figure 9, an image of the white pine crib after extinction.

Figure 9. Fully extinct wood crib.

During trial burns, white pine reached a steady-state burning rate quicker than the HPDE,

PVC, and neoprene rubber cribs. This was likely the result of no additional radiative heat being

required to reach the flashpoint of additional (non-wood) materials within the fuel package.

Wood burning is based on pyrolysis (i.e. thermal decomposition) of cellulose and the reactions of

the pyrolysis products with each other along with gasses—primarily oxygen (InnooFireWood,

n.d). It is largely due to pine wood's production of substances that easily react with oxygen that a

steady burning rate with non-turbulent flame production was generated within the least amount

of time compared to other crib compositions.

4.4 High Density Polyethylene Burn Analysis

The High Density Polyethylene (HDPE) crib was designed with 75% white pine sticks and 25% HDPE sticks. Within seconds of the heptane pool fire burning out, the HDPE crib appeared to be fully ignited, which none of the other cribs, except for the white pine crib, did. Approximately 300 seconds into the burn the HPDE crib reached the beginning of its steady-state mass loss duration. At this point, the HDPE sticks turned from white to black and began to drip, eventually creating a steady stream of melted plastic flowing in the aluminum collection tray. The steady flowing of the HDPE into the collection tray further indicated steady mass loss rate per unit time. Throughout combustion and suppression, the crib released white smoke and occasionally when the water droplets from the suppression system hit the crib, white particulates sprayed from the sides of the crib. This process continued throughout steady-state burning of the HDPE crib. At approximately 4 minutes into the burn, 90% of the HDPE had burned and dripped into the collection tray (Figure 10).

Figure 10. Fully extinct HDPE crib.

Due to its thermoplastic nature, HDPE was found to be highly flammable in comparison to the neoprene rubber and PVC polymeric materials burned. The HDPE dripped due to the intermolecular force acting between polymers weakening on heating. The neoprene rubber and

`

PVC polymers did not drip from their cribs because they are thermosets. Because HDPE has a lower melting point than neoprene rubber and PVC, the crib was able to fully ignite in a shorter period of time. Overall, the radiative heat flux required for HDPE to combust was fulfilled in a shorter period of time compared to the neoprene rubber and PVC cribs.

4.5 PVC Burn Analysis

The combustion of the PVC crib was designed with 75% of the sticks being white pine wood and 25% of the sticks being PVC. As a thermoset, a material which is cured (heated) to set, PVC becomes more rigid and brittle when exposed to heat. Due to the high thermal conductivity of PVC, it took approximately 375 sec to reach the crib's steady-state burning period—the longest of the four crib compositions. The crib also produced a high amount of smoke both throughout the burn as well as after suppression. The crib was also suppressed quickly, approximately 15 seconds during both trials, in contrast to the 30-45 seconds for the white pine wood, HDPE, and neoprene rubber. As it burned, the PVC puffed up; a bubbly, char-like layer formed on the PVC, and a reflective layer was observed underneath. This can be seen in Figure 11, an image of the PVC crib after extinction.

Figure 11. Fully extinct PVC crib.

PVC is not considered to have excellent fire performance, meaning that it will only burn when exposed to a certain heat flux. While the necessary heat flux will certainly be present in an environment such as a house fire, PVC itself does not readily ignite (Hirschler, 2017). This difficulty in igniting PVC contributes to the high amount of smoke observed. Smoke originates from particles of the material not being able to ignite due to insufficient energy, heat, fuel, or oxygen. PVC produced more smoke as it is a harder material to ignite, requiring temperatures beyond 390°C to ignite (Uitenham et al., 1981).

4.6 Neoprene Rubber Burn Analysis

The combustion of the neoprene rubber crib was designed with 75% of the sticks being white pine wood and 25% of the sticks being neoprene rubber. The crib took approximately 245 seconds to fully ignite from the heptane pool fire, with the flames slowly spreading from the back of the crib to the front before reaching steady state. The smoke that eventually developed was dark. After the water suppression system was activated, the smoke produced was white; this white smoke continued until the suppression system was stopped. The neoprene rubber sticks were extinguished by the water but did not visibly change with the addition of water. Following extinction, the neoprene rubber was charred and brittle, similar to the white pine wood after complete combustion, except for the minor expansion of the neoprene rubber sticks (Figure 12).

`

Figure 12. Fully extinct neoprene rubber crib.

The neoprene rubber expanded during combustion because the heat from the fire raised the neoprene rubber sticks' entropy allowing it to expand and stretch. Similar to PVC, neoprene rubber is a thermoset, requiring elevated levels of radiant heat flux to fully combust and ignite. However, neoprene rubber repeatedly reached its steady-state burning duration quicker than PVC and continuously had an average steady-state mass loss rate approximately two-fold that of PVC. These two contrasts can be attributed to neoprene rubber's flash point of approximately 500°F, around 234 degrees less than that of PVC's flash point (Waller, 2000). Additionally, neoprene exhibited other overlapping qualities to PVC, such as becoming rigid and brittle, and increasing its surface area and expanding under intense heat.

Water samples collected during the neoprene rubber, PVC, white pine wood, HDPE, and combustion/suppression trials were varying shades of yellow, including, in some cases, samples from the same type of crib.

`

4.7 GC-MS Standard Data

To determine concentrations of the indicator chemicals in each tested sample, standard curves were created using known standards: Supelco EPA 625 Semivolatile Calibration Mix and Supelco EPA 502/524 Volatiles Organic Calibration Mix (without gasses), each at concentrations of 0.1, 1, and 10 ppb. Figure 13 includes the standard curves for five out of the six indicator chemicals.
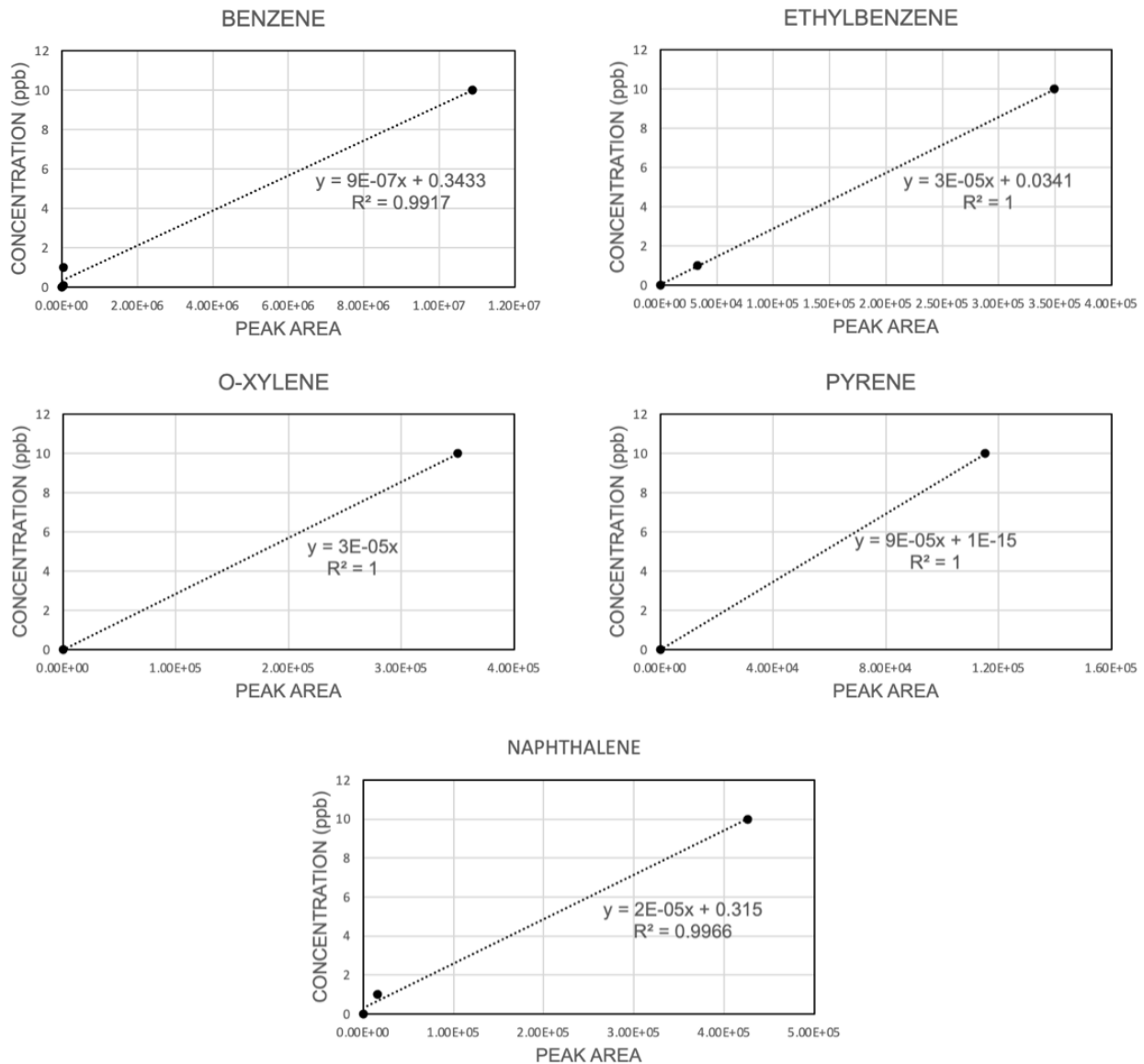
Figure 13. Standard curves of indicator chemicals: benzene, ethylbenzene, o-xylene, pyrene, and naphthalene.

Three volatile organic compounds (VOCs) (benzene, ethylbenzene, and o-xylene) and three polyaromatic hydrocarbons (PAHs) (pyrene, naphthalene, and anthracene) were chosen as indicator chemicals. Standard curves for all of the VOCs and two of the PAHs were created. The GC-MS was unable to detect the indicator chemicals at 0.1 and 1 ppb for most of the samples, resulting in nonideal and less accurate standard curves due to limited points. Additionally,

anthracene, along with many of the known PAHs in EPA 625, did not appear on any of the GC-MS chromatograms produced. Further investigation should be conducted to determine the cause.

4.8 GC-MS Sample Data

The table and histogram below lists the parts per billion of each indicator chemical present in the water samples collected after burn suppression. The chromatogram below for the PVC 1 sample, labeled as Figure 14, shows an example of the results collected from the GC-MS after running the water samples, indicating the different contaminants detected in the sample. A complete set of chromatographs can be found in Appendix D. Each of the blue peaks identifies a different compound detected by the GC-MS. As seen in the graph, benzene, pyrene and naphthalene are the indicators found in the PVC 1 sample. There are several other identifiable peaks found on this chromatogram and with further research these may be identified.
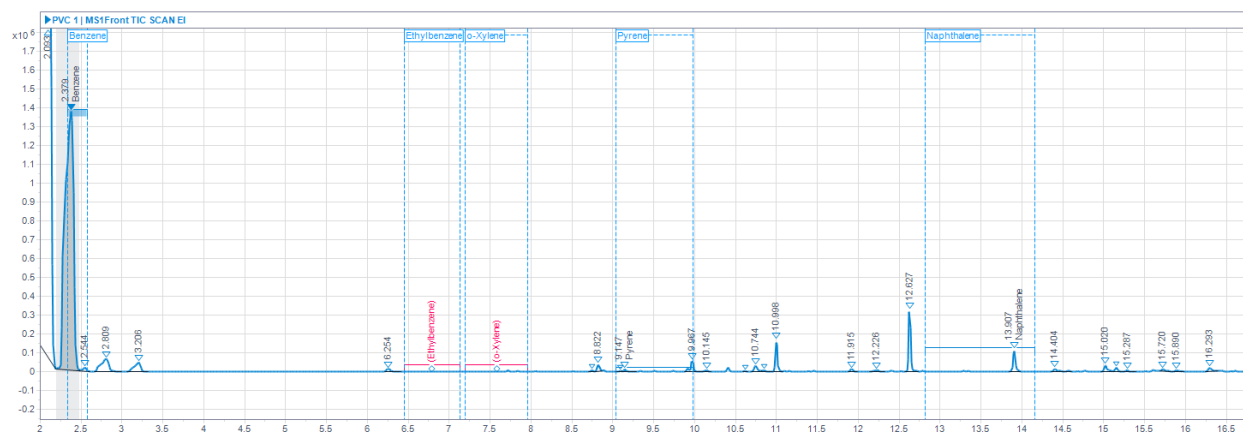
Figure 14. Chromatogram for the PVC 1 sample.

The concentrations were also calculated from the GC-MS data of each water sample on the y-axis of the chromatograph, depending on how high each peak is. Unlike the other three indicators, o-xylene was only found in the water sample from the first rubber burn. Benzene, pyrene, and naphthalene are consistently present in the water samples because these molecules are commonly found in plastics and rubbers, and are known to be by-products of incomplete combustion reactions. The increase in benzene concentration in HDPE, PVC, and rubber compared to white pine correlates with this contaminant having a greater presence in polymers than in plants such as white pine trees. The concentration of pyrene consistently decreases for

35

`

each material's two burns. Pyrene's higher concentration in the first burn of each sample could be a result of less complete combustion reactions in the first burn than in the second. Naphthalene follows a similar pattern to pyrene, except for the case of HDPE. Ethylbenzene was not detected in any of the other water samples, so it was not listed with the other contaminants in Figure 15 and Table 4.
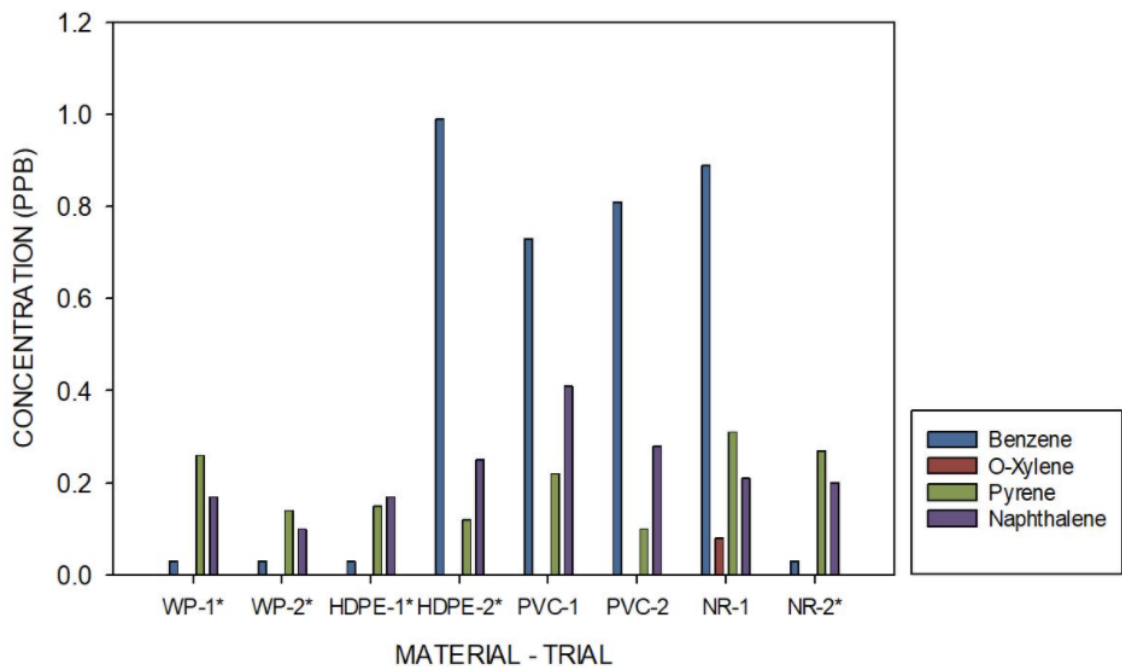
Figure 15. Histogram of the contaminant concentrations in all eight burn samples.
* indicates samples were reconstituted and may have lower concentrations of volatiles.

`

Table 4. Concentrations of each indicator chemical from water samples of all eight burns. Ethylbenzene was not detected in any of the water samples and dashes indicate that contaminant was not detected in the sample.

Concentration in Water Samples (ppb)

Material	Burn Number	Benzene	O-Xylene	Pyrene	Naphthalene
White Pine*	1	0.03	-	0.26	0.17
White Pine*	2	0.03	-	0.14	0.10
HDPE*	1	0.03	-	0.15	0.17
HDPE*	2	0.99	-	0.12	0.25
PVC	1	0.73	-	0.22	0.41
PVC	2	0.81	-	0.10	0.28
Rubber	1	0.89	0.08	0.31	0.21
Rubber*	2	0.03	-	0.27	0.20

*Samples that evaporated and were reconstituted

As indicated with the asterisks in the table above, the white pine 1, white pine 2, HDPE 1, HDPE 2, and rubber 2 burns were the five samples that almost completely evaporated due to the volatility of methylene chloride and lack of proper sealing. The methods described in section 3.10 were performed on these samples with new methylene chloride and were then properly sealed. The reconstitution proved to be effective because at least some amount of contaminants were detected. However, it is likely that the concentrations of these contaminants were lower than they would have been in the original samples because some of the contaminants could have evaporated with the methylene chloride. This is clearly demonstrated between the two rubber burns. Rubber 1 had a significantly higher concentration of benzene compared to rubber 2, which was a sample that evaporated and was reconstituted.

As discussed previously, determining the beginning and end point of a secondary steady state was difficult to do in real time with the LabView software, as the collection of water droplets would increase the total mass. This, as well as inconsistencies in the rate of water application rate, would likely have affected contaminant concentrations and the water volume

captured for each sample. It should also be noted that a general correlation can be made between (1) mass loss rates during preliminary steady-state trials and (2) longer suppression and secondary steady state durations during suppression trials with the chemical concentrations in the collected water samples. Crib compositions experiencing greater mass loss rates and longer suppression and secondary steady state durations typically exhibited higher chemical concentrations.

4.9 Sample Data Discussion

4.9.1 Comparison to Literature

The collected results are consistent with literature in the contaminants identified, but the contaminant concentrations were significantly lower, as shown in Table 5.

Table 5. Comparison of concentration of naphthalene vs. literature. The concentration of Naphthalene in aqueous samples from literature under similar laboratory conditions is a factor of 5 magnitudes higher than calculated values, based on the study by Valavanidis et al. (2008).

Sample Material	Concentration of Naphthalene [ppb]	Literature Concentration of Naphthalene [ppb] (Valavanidis et al. 2008)
PVC	0.28-0.41	80000 ± 9000
HDPE	0.17-0.25	23000 ± 4000

Concentrations of naphthalene from PVC and HDPE plastics burned in water in similar laboratory settings were 5 magnitudes higher than the currently collected samples (Valavanidis et al. 2008). This trend continues with other detected indicator chemicals, most notably benzene (Isaacson, 2020) being found at 0.5 ppm as an aqueous phase contaminant vs. the detected range of .03-.99 ppb, a 3-4 magnitude difference. It should be noted, both the Valavanidis and Isaacson studies samples analyzed in the GC-MS were diluted or leached with distilled water following the collection and isolation of residue ash and particulate soot following the combustion of natural and polymer materials. This study's methodology relied on the collection of contaminants through the suppression of a thermally degrading material at steady state over a time period of less than 200 seconds. This study used a much shorter contact time, thus resulting in less possible mass transfer.

`

Two selected indicator chemicals for which concentrations were calculated—ethylbenzene and anthracene—did not appear in any samples, while o-xylene only appeared in the rubber 2 sample at a concentration of 0.08 ppb. Additionally, other PAHs known to leach into water from burning plastics were not detected, such as chrysene, benzo[a]pyrene, and acenaphthene.

The low concentrations and lack of detection of expected contaminants are likely due to a major error in storage of the samples—the evaporation of five of the eight samples lead to the destruction and reduction in concentration of more volatile contaminants. This is a possible source of error and explanation for the difference in our results and the expected results from literature.

4.9.2 Possible Other Contaminants in the Samples

While the concentrations of indicator chemicals was lower than expected, other additional peaks were identified indicating chemicals consistent with literature. Table 6 includes a sample list of additional contaminants identified via the GC-MS management software library with a greater than 60% probability of being the chemical identified. The full table on a sample by sample basis with the probabilities can be found in appendix E.

Table 6. List of potential contaminants as identified by the GC-MS library per sample, and compared to several sources (Lam et al., 2020; Valavanidis et al., 2008; Chong et al., 2019).

Retention Time	Contaminant	Samples				
		White Pine	HDPE	PVC	Neoprene Rubber	In literature
1.936-1.952	3-methylpentane	✓		✓		
2.085-2.103	n-Hexane	✓	✓	✓	✓	✓
2.544-2.552	Amylene Hydrate		✓	✓	✓	
2.798-2.818	Cyclohexane	✓	✓		✓	
5.33	Cyclopentanone				✓	
6.256	2-oxo-3-cyclopentene-1-acetaldehyde				✓	
8.746-8.747	Benzaldehyde			✓	✓	✓
9.967-9.972	2-ethyl-1-hexanol			✓		✓
10.998-11.004	2-methoxyphenol	✓	✓	✓	✓	✓
11.368-11.369	6,7-dihydro-5H-1-pyrindine				✓	✓
12.629-12.630	2-methoxy-4-methylphenol	✓	✓			✓
13.132-13.113	Benzothiazole				✓	
13.814	3-Ethyl-5,6,7,8-tetrahydroquinoline				✓	
13.905-13.907	4-ethyl-2-methoxyphenol				✓	
14.149-14.151	2-methyl-benzothiazole				✓	✓
15.155	2-methoxy-4-phenol	✓				✓
15.156-15.158	2-methoxy-4-propylphenol	✓	✓	✓		
19.072-19.076	4-hydroxy-3-methoxy-benzenepropanol			✓	✓	✓

Two potential contaminants were detected in all sample types: 2-methoxyphenol and n-hexane, both appearing in the literature (Lam et al., 2020), with several others appearing in at least three sample types. Additional possible contaminants not previously identified in literature—such as 2-methoxy-4-propylphenol, cyclohexane, and amylene hydrate—were present in at least four samples. Future research can begin to quantify the concentrations that appear in run-off through similar methods as with the indicator chemicals.

4.10 EPA Maximum Contaminant Levels of Detected Contaminants

The EPA has published Maximum Contaminant Levels (MCLs) for three of the four indicators detected in the samples. The current effluent limitations of benzene, pyrene, o-xylene and naphthalene are seen below in Table 7. These values are daily maxima, as volatile and semi-volatile organic molecules pose a number of health risks. Benzene is known to be highly hazardous, as it has an EPA cancer classification of Group A: known human carcinogens. However, pyrene has neither been proven or disproven to be a human carcinogen, and is listed as a Group D chemical: not classifiable as to human carcinogenicity. All molecules in the xylene family are classified in Group D as well, and naphthalene is in Group C: possibly carcinogenic to humans. While these contaminants are not all known carcinogens, they do share some other types of hazards. The most common of these are headaches, fatigue, dizziness, tremors, and possible kidney effects.

Table 7. Discharge limit for each detected contaminant.

Contaminant	Discharge limit (µg/L)
Benzene	5.0
Pyrene	100*
O-xylene	100**
Naphthalene	20

* Total Discharge limit for Group II Polycyclic Aromatic Hydrocarbons
** Collective Discharge limit for Benzene, Toluene, Ethylbenzene, and total Xylenes.

5.0 Conclusions and Recommendations

This project achieved its goals using several chemical techniques and engineering strategies. Prior to experimentation, the team researched materials commonly known to produce harmful contaminants when burned, and incorporated these substances into the cribs. The materials and structure of the crib and the design of the suppression system were crucial to the safety, repeatability, and efficiency of the combustion and suppression procedures. The data

`

obtained from the GC-MS identified each contaminant in the water samples and quantified their concentrations.

It is recommended that future research of contaminant mobilization employ a larger number of indicator chemicals and use more water during the extraction process. Additional indicators will allow for more standard curves to identify peaks in the experimental curves, and a larger volume of water will improve the quality of the data obtained during extraction. Many compounds used in this study are highly volatile, and can almost entirely evaporate if left unsealed and unfrozen for long periods of time. It is strongly suggested that samples are sealed in an airtight container and refrigerated if freezing is not an option. As a crucial aspect of this experiment, the GC-MS should be set up to ensure maximum efficiency. Given this, research on why PAHs and semivolatiles did not appear is necessary to find the sources of error in this project. Ash particulates and aqueous contaminants should also be taken into account when the procedure is carried out and the data is analyzed.

Lastly, it is also recommended that future work should improve the current design of the suppression system, to provide a more consistent water application rate to selected fuel package materials, or design a suppression method to further increase the contact time between combustion byproducts and the suppression water. This will provide future teams with more accurate predictions of collected water volumes, reduced fluctuation in mass loss data, and likely increase contaminant concentrations based on results from previous studies (Valavanidis et al., 2008).

While this is one option, it is also encouraged that a variety of other suppression methods to induce controlled mass transfer phenomena in suppression samples are researched and applied. This, alongside the selecting a wider range of materials typically involved in residential fire events, will also be necessary as this project progresses, to provide more data for current research in the field of contaminant mobilization and resiliency efforts as fire events increase due to climate change.

References:

Abatzoglou, J. T., & Williams, A. P. (2016). Impact of anthropogenic climate change on wildfire across western US forests. Proceedings of the National Academy of Sciences, 113(42), 11770-11775. https://doi.org/10.1073/pnas.1607171113

Anderson, J. (2019). Polycyclic Aromatic Hydrocarbon Release from Pavement Rejuvenators Due to Rolling Wheel Contact: An Investigation Using a Model Mobile Load Simulator (Unpublished master's thesis). Worcester Polytechnic Institute.

Aracil, I., Font, R., & Conesa, J. A. (2005). Semivolatile and volatile compounds from the pyrolysis and combustion of polyvinyl chloride. Journal of analytical and applied pyrolysis, 74(1-2), 465-478. https://doi.org/10.1016/j.jaap.2004.09.008

ASTM International. (2019). Standard Practice for Separation of Ignitable Liquid Residues from Fire Debris Samples by Solvent Extraction (ASTM E1386-15). Retrieved from https://www.astm.org/e1386-15.html

Balch, J. K., Bradley, B. A., Abatzoglou, J. T., Nagy, C. R., Fusco, E. J., & Mahood, A. L. (2017, March 14). Human-started wildfires expand the fire niche across the United States. PNAS. https://www.pnas.org/content/114/11/2946

Busse, M. D., Hubbert, K. R., Fiddler, G. O., Shestak, C. J., & Powers, R. F. (2005). Lethal soil temperatures during burning of masticated forest residues. International Journal of Wildland Fire, 14(3), 267-276. https://doi.org/10.1071/WF04062

California Department of Fish and Wildlife. (2022). Science: Wildfire impacts. CDFW. Retrieved January 14, 2022, from https://wildlife.ca.gov/Science-Institute/Wildfire-Impacts

California Water Boards. (2018). Maximum Contaminant Levels And Regulatory Dates for Drinking Water: U.S. EPA vs California. https://www.waterboards.ca.gov/drinking_water/certlic/drinkingwater/documents/ccr/mcls_epa_vs_dwp.pdf.

Chong, N. S., Abdulramoni, S., Patterson, D., & Brown, H. (2019). Releases of Fire-Derived Contaminants from Water Pipes Made of Polyvinyl Chloride Polymer. doi: 10.20944/preprints201909.0281.v1

`

Chudy, R. P., & Hagler, R. W. (2020). Dynamics of global roundwood prices–Cointegration

　　　　analysis. Forest Policy and Economics, 115, 102155.

　　　　https://doi.org/10.1016/j.forpol.2020.102155

County of Santa Cruz. (2020). Water Wells and Springs, Santa Cruz, California.

　　　　https://www.santacruzcounty.us/Portals/6/Env_Health/CZU_Fire/WaterWellFireReturn.p

　　　　df.

DeWeerdt, S. (2021, August 9). Humans cause almost all wildfires that threaten homes in the S.

　　　　Anthropocene. https://www.anthropocenemagazine.org/2020/09/humans-cause-most-

　　　　wildfires-that-threaten-homes-in-the-united-states/

Environmental Protection Agency (2003, July) Contaminant Candidate List Regulatory

　　　　Determination Support Document for Naphthalene.

　　　　https://www.epa.gov/sites/default/files/2014-09/documents/support_cc1_naphthalene_

　　　　ccl_regdet.pdf

Fent, K. W., Evans, D. E., Babik, K., Striley, C., Bertke, S., Kerber, S., Smith, D., & Horn, G. P.

　　　　(2018). Airborne contaminants during controlled residential fires. Journal of

　　　　Occupational and Environmental Hygiene, 15(5), 399–412.

　　　　https://doi.org/10.1080/15459624.2018.1445260

Fischer, E. C., & Varma, A. H. (2016, September). Environmental impacts of fire. STRUCTURE

　　　　magazine. https://www.structuremag.org/?p=10431

Folkman, S. (2018). Water Main Break Rates In the USA and Canada: A Comprehensive Study.

　　　　Mechanical and Aerospace Engineering Faculty Publications. Paper 174.

　　　　https://digitalcommons.usu.edu/mae_facpub/174

Hirschler, M. (2017). Fire Properties of Polyvinyl Chloride. Vinylinfo.Org. GBI International,

　　　　Consultant of The Vinyl Institute https://www.vinylinfo.org/wp-

　　　　content/uploads/2018/12/Fire-Properties-of-Polyvinyl-Chloride_0.pdf

InnoFireWood. (n.d.). Innovative eco-efficient high fire performance wood products for

　　　　demanding applications. Burning of wood.

　　　　http://virtual.vtt.fi/virtual/innofirewood/stateoftheart/database/burning/burning.html#:~:te

　　　　xt=Under%20the%20influence%20of%20heat,wood%20to%20ignite%20and%20burn.&

　　　　text=Gaseous%20substances%20react%20with%20each,induces%20pyrolysis%20and%

　　　　20combustion%20reactions

`

Isaacson, K. P., Proctor, C. R., Wang, Q. E., Edwards, E. Y., Noh, Y., Shah, A. D., & Whelton, A. J. (2021). Drinking water contamination from the thermal degradation of plastics: implications for wildfire and structure fire response. Environmental Science: Water Research & Technology, 7(2), 274-284. DOI: 10.1039/D0EW00836B

Kizer, K. W. (2020). Extreme wildfires—a growing population health and planetary problem. Jama, 324(16), 1605-1606. DOI: 10.1001/jama.2020.19334

Kung, H., & Hill, J.P. (1975). Extinction of wood crib and pallet fires. *Combustion and Flame, 24*, 305-317.

Lam, R., Lennard, C., Kingsland, G., Johnstone, P., Symons, A., Wythes, L., ... & Spikmans, V. (2020). Rapid on-site identification of hazardous organic compounds at fire scenes using person-portable gas chromatography-mass spectrometry (GC-MS)–part 2: water sampling and analysis. Forensic sciences research, 5(2), 150-164. https://doi.org/10.1080/20961790.2019.1662648

Loganathan, G. V., & Lee, J. (2005). Decision tool for optimal replacement of plumbing systems. Civil Engineering and Environmental Systems, 22(4), 189-204. https://doi.org/10.1080/10286600500279964

Lomnicki, S., Gullett, B., Stöger, T., Kennedy, I., Diaz, J., Dugas, T. R., Varner, K., Carlin, D. J., Dellinger, B., & Cormier, S. A. (2014). Combustion by-products and their health effects—Combustion Engineering and Global Health in the 21st Century. International Journal of Toxicology, 33(1), 3–13. https://doi.org/10.1177/1091581813519686

Magee, R. S., & Reitz, R. D. (1975, January). Extinguishment of radiation augmented plastic fires by water sprays. In Symposium (International) on Combustion (Vol. 15, No. 1, pp. 337-347). Elsevier. https://doi.org/10.1016/S0082-0784(75)80309-2

Martin, D., Tomida, M., & Meacham, B. (2016). Environmental impact of fire. Fire Science Reviews, 5(1), 1-21. https://doi.org/10.1186/s40038-016-0014-1

McAllister, S., & Finney, M. (2015, October 12). The Effect of Wind on Burning Rate of Wood Cribs. Retrieved January 20, 2022, from https://link.springer.com/article/10.1007%2Fs10694-015-0536-4

Murphy, S. F., Writer, J. H., McCleskey, R. B., & Martin, D. A. (2015). The role of precipitation type, intensity, and spatial distribution in source water quality after wildfire. Environmental Research Letters, 10(8), 084007. doi:10.1088/1748-9326/11/7/079501

Pacific Northwest Research Station. (2021). Pacific Northwest Research Station. Fire Effects on
the Environment | Pacific Northwest Research Station | PNW-US Forest Service.
https://www.fs.usda.gov/pnw/page/fire-effects-environment

Paradise Irrigation District. (2019). Paradise Annual Consumer Confidence Report, Paradise.
https://pidwater.com/docs/about-your-water/water-quality/1750-2019-consumer-
confidence-report/file.

Proctor, C. R., Lee, J., Yu, D., Shah, A. D., & Whelton, A. J. (2020). Wildfire caused widespread
drinking water distribution network contamination. AWWA Water Science, 2(4), e1183.
https://doi.org/10.1002/aws2.1183

Quintiere, J. G., Carey, A. C., Reeves, L., & McCarthy, L. K. (2017, June). Scale modeling in
Fire Reconstruction-Ojp.gov. Scale Modeling in Fire Reconstruction.
https://www.ojp.gov/pdffiles1/nij/grants/250920.pdf.

Radeloff, V. C., Hammer, R. B., Stewart, S. I., Fried, J. S., Holcomb, S. S., & McKeefry, J. F.
(2005, June 1). The wildland-urban interface in the United States. The Ecological Society
of America. https://esajournals.onlinelibrary.wiley.com/doi/full/10.1890/04-1413

Resources, W. (2019, March 1). Water quality after wildfire active. Water Quality After Wildfire
| U.S. Geological Survey. https://www.usgs.gov/mission-areas/water-
resources/science/water-quality-after-wildfire

Rockaway, T. D., Willing, G. A., & Nagisetty, R. M. (2007). Life predictions of elastomers in
drinking water distribution systems. Journal-American Water Works Association, 99(12),
99-110. https://doi.org/10.1002/j.1551-8833.2007.tb08113.x

Shemwell, B. E., & Levendis, Y. A. (2000). Particulates generated from combustion of polymers
(plastics). Journal of the Air & Waste Management Association, 50(1), 94-102.
https://doi.org/10.1080/10473289.2000.10463994

Simoneit, B. R., Medeiros, P. M., & Didyk, B. M. (2005). Combustion products of plastics as
indicators for refuse burning in the atmosphere. Environmental science & technology,
39(18), 6961-6970. https://doi.org/10.1021/es050767x

Smith H. G., et al., Wildfire effects on water quality in forest catchments: A review with
implications for water supply, Journal of Hydrology, Volume 396, Issues 1–2, 2011,
Pages 170-192, https://doi.org/10.1016/j.jhydrol.2010.10.043.

`

Spearing, L. A., & Faust, K. M. (2020). Cascading system impacts of the 2018 Camp Fire in California: the interdependent provision of infrastructure services to displaced populations. International Journal of Disaster Risk Reduction, 50, 101822. https://doi.org/10.1016/j.ijdrr.2020.101822

Speight, J. G. (2020). Handbook of Industrial Hydrocarbon Processes (2nd ed.). Gulf Professional Publishing, an imprint of Elsevier.

Stenstrom, M. K., & Kayhanian, M. (2005). First flush phenomenon characterization (No. CTSW-RT-05-073.02. 6). California Department of Transportation Division of Environmental Analysis.

Ueno, T., Nakashima, E., & Takeda, K. (2010). Quantitative analysis of random scission and chain-end scission in the thermal degradation of polyethylene. Polymer degradation and stability, 95(9), 1862-1869. https://doi.org/10.1016/j.polymdegradstab.2010.04.020

Uitenham, L. C., & Geil, P. H. (1981). Processing, morphology, and properties of PVC. Journal of Macromolecular Science, Part B: Physics, 20(4), 593-622

U.S. Environmental Protection Agency. (2018). Edition of the Drinking Water Standards and Health Advisories Tables. https://www.epa.gov/sites/default/files/2018-03/documents/dwtable2018.pdf

Valavanidis, A., Iliopoulos, N., Gotsis, G., & Fiotakis, K. (2008). Persistent free radicals, heavy metals and pahs generated in particulate soot emissions and residue ash from controlled combustion of common types of plastic. Journal of Hazardous Materials, 156(1-3), 277–284. https://doi.org/10.1016/j.jhazmat.2007.12.019

Vanderbilt Chemistry Department. Vacuum Filtration. Vanderbilt University. Retrieved from https://www.vanderbilt.edu/AnS/Chemistry/courses/chem104/experiment2/vacuum/vacuum2.htm

Waller, J. M., Haas, J. P., & Beeson, H. D. (2000). Polymer-Oxygen Compatibility Testing: Effect of Oxygen Aging on Ignition and Combustion Properties. ASTM SPECIAL TECHNICAL PUBLICATION, 1395, 73-86.

Whelton A. J., Proctor C., Lee J., & Shah A. D. (2019). VOC Fate in Water Systems Discussion to Support the Water Plumbing. https://engineering.purdue.edu/PlumbingSafety/resources/Camp-Fire-VOC-in-Water-Systems-Purdue.pdf.

`

Whelton, A. J., Shah , A., & Isaacson, K. P. (2022, January 11). Plastic pipes are polluting drinking water systems after wildfires—it's a risk in urban fires, too. The Conversation. https://theconversation.com/plastic-pipes-are-polluting-drinking-water-systems-after-wildfires-its-a-risk-in-urban-fires-too-150923

Yu, J., Sun, L., Ma, C., Qiao, Y., & Yao, H. (2016). Thermal degradation of PVC: A review. Waste Management (Elmsford), 48, 300–314. https://doi.org/10.1016/j.wasman.2015.11.041

Zhang, Y., & Wang, Y. (2010). Impact of environmental pollution. Impact, monitoring and management of environmental pollution. New York (NY): Nova Science Publishers, Inc.

`

Appendices

Appendix A

Narrowed down list of expected contaminants in water
Polyaromatic hydrocarbons

Acenaphthene	Benzo[g,h,i]perylene	Indeno[1,2,3-cd]pyrene
Anthracene	Benzo[k]fluoranthene	Irganox 1010 Constituent
Benzo[a]anthracene	Chrysene	Naphthalene
Benzo[a]pyrene	Dibenzo[a,h]anthracene	Phenanthrene
Benzo[b]fluoranthene	Fluorene	Pyrene

Volatile Organic Compounds

Benzene	Ethyl Benzene	Methylpentane isomer
1-butene	2-ethyl-1-hexanol	Octadecane
1,3-butadiene	Formaldehyde	N-pentane
2-butoxyethanol	N-hexane	Trimethylamine
Dimethylbutane Isomer	Hexadecane	Tetradecane
Dimethyloctane Isomer	Methylbutadiene isomer	Toluene
Docosane	Methylbutane isomer	Xlyenes

Appendix B

Standards list and concentrations
Supelco EPA 625 Semivolatile Calibration Mix
1000 µg/mL each component in methylene chloride: benzene (3:1)

Acenaphthene	2-Chlorophenol	Hexachlorocyclopentadiene
Acenaphthylene	Chrysene	Hexachloroethane
Anthracene	Dibenz[a,h]anthracene	Indeno[1,2,3-cd]pyrene
Azobenzene	Dibutyl phthalate	Isophorone
Benz[a]anthracene	1,2-Dichlorobenzene	2-Methyl-4,6-dinitrophenol
Benzo[b]fluoranthene	1,3-Dichlorobenzene	Naphthalene
Benzo[k]fluoranthene	1,4-Dichlorobenzene	Nitrobenzene
Benzo[ghi]perylene	2,4-Dichlorophenol	2-Nitrophenol
Benzo[a]pyrene	Diethyl phthalate	4-Nitrophenol
Benzyl butyl phthalate	2,4-Dimethylphenol	N-Nitrosodimethylamine
Bis(2-chloroethoxy)methane	Dimethyl phthalate	N-Nitrosodi-n-propylamine
Bis(2-chloroethyl) ether	2,4-Dinitrophenol	Pentachlorophenol
Bis(2-ethylhexyl) phthalate	2,4-Dinitrotoluene	Phenanthrene
4-Bromodiphenyl ether	2,6-Dinitrotoluene	Phenol
Carbazole	Di-n-octyl phthalate	Pyrene
4-Chlorodiphenyl ether	Fluoranthene	1,2,4-Trichlorobenzene
Bis-(2-chloroisopropyl) ether	Fluorene	2,4,6-Trichlorophenol
4-Chloro-3-methylphenol	Hexachlorobenzene	
2-Chloronaphthalene	Hexachloro-1,3-butadiene	

Supelco EPA 502/524 Volatiles Organic Calibration Mix (without gasses)
2000 μg/mL each component in methanol

Benzene	1,3-Dichlorobenzene	Naphthalene
Bromobenzene	1,4-Dichlorobenzene	Propylbenzene
Bromochloromethane	1,1-Dichloroethane	Styrene
Bromodichloromethane	1,2-Dichloroethane	1,1,1,2-Tetrachloroethane
Bromoform	1,1-Dichloroethylene	1,1,2,2-Tetrachloroethane
Butylbenzene	cis-1,2-Dichloroethylene	Tetrachloroethylene
sec-Butylbenzene	trans-1,2-Dichloroethylene	Toluene
tert-Butylbenzene	Dichloromethane	1,2,3-Trichlorobenzene
Carbon tetrachloride	1,2-Dichloropropane	1,2,4-Trichlorobenzene
Chlorobenzene	1,3-Dichloropropane	1,1,1-Trichloroethane
Chloroform	2,2-Dichloropropane	1,1,2-Trichloroethane
2-Chlorotoluene	1,1-Dichloro-1-propene	Trichloroethylene
4-Chlorotoluene	cis-1,3-Dichloropropene	1,2,3-Trichloropropane
Dibromochloromethane	trans-1,3-Dichloropropene	1,2,4-Trimethylbenzene
1,2-Dibromo-3-chloropropane	Ethylbenzene	Mesitylene
1,2-Dibromoethane	Hexachloro-1,3-butadiene	m-Xylene
Dibromomethane	Cumene	o-Xylene
1,2-Dichlorobenzene	p-Cymene	p-Xylene

Appendix C

Expected outputs from Pro EZCG Chromatogram Modeler
(https://www.restek.com/en/technical-literature-library/brands/EZGC-online-tools/)
Supelco EPA 625 Semivolatile Calibration Mix

Peaks	Retention Time (min)	Resolution	Peak Width (min)	Temperature (°C)
N-Nitrosodimethylamine	4.52	133	0.037	45.2
Phenol	9.42	4.2	0.035	94.2
bis-(2-chloroethyl)ether	9.56	1.4	0.035	95.6
2-Chlorophenol	9.61	1.4	0.036	96.1
1,3-Dichlorobenzene	9.94	4.3	0.037	99.4
1,4-Dichlorobenzene	10.1	4.3	0.037	101
1,2-Dichlorobenzene	10.42	8.7	0.037	104.2
Bis(2-Chloroisopropyl)ether	10.74	7.6	0.035	107.4
N-Nitrosodi-N-propylamine	11.01	3.8	0.035	110.1
Hexachloroethane	11.15	3.8	0.038	111.5
Nitrobenzene	11.31	4.2	0.037	113.1
Isophorone	11.87	4.4	0.036	118.7
2-Nitrophenol	12.03	4.4	0.037	120.3
2,4-Dimethylphenol	12.23	5.4	0.035	122.3
Bis(2-chloroethoxy)methane	12.44	4.2	0.035	124.4
2,4-Dichlorophenol	12.59	4.2	0.037	125.9
1,2,4-Trichlorobenzene	12.77	3.8	0.037	127.7
Naphthalene	12.92	3.8	0.038	129.2
Hexachloro-1,3-Butadiene	13.29	9.9	0.037	132.9
4-Chloro-3-methylphenol	14.31	18.2	0.036	143.1
Hexachlorocyclopentadiene	14.96	7.4	0.038	149.6
2,4,6-Trichlorophenol	15.24	7.4	0.038	152.4
2-Chloronaphthalene	15.66	10.9	0.038	156.6
Dimethyl phthalate	16.48	2.2	0.037	164.8
2,6-Dinitrotoluene	16.56	1.5	0.037	165.6
Acenaphthylene	16.62	1.5	0.039	166.2
Acenaphthene	17.04	3.2	0.04	170.4

2,4-Dinitrophenol	17.17	3.2	0.038	171.7
4-Nitrophenol	17.42	1.9	0.037	174.2
2,4-Dinitrotoluene	17.49	1.9	0.038	174.9
Diethyl Phthalate	18.17	2.2	0.037	181.7
Fluorene	18.26	1.9	0.04	182.6
4-Chlorodiphenyl ether	18.33	1.9	0.038	183.3
2-Methyl-4,6-dinitrophenol	18.44	2.7	0.039	184.4
Azobenzene	18.7	6.6	0.039	187
4-Bromodiphenyl ether	19.47	2.3	0.039	194.7
Hexachlorobenzene	19.56	2.3	0.04	195.6
Pentachlorophenol	20.05	11	0.041	200.5
Phenanthrene	20.5	2.9	0.041	205
Anthracene	20.62	2.9	0.041	206.2
Carbazole	21.05	10.5	0.041	210.5
Dibutyl phthalate	22.08	25.3	0.038	220.8
Fluoranthene	23.3	12	0.043	233
Pyrene	23.81	12	0.043	238.1
Benzyl butyl phthalate	25.6	26.8	0.04	256
Benz[a]anthracene	26.67	1.8	0.043	266.7
Chrysene	26.75	1.8	0.044	267.5
Bis(2-ethylhexyl) phthalate	27.07	7.1	0.039	270.7
Di-n-octyl phthalate	28.52	13.2	0.04	285.2
Benzo[b]fluoranthene	29.04	1.2	0.045	290.4
Benzo[k]fluoranthene	29.1	1.2	0.045	291
Benzo[a]pyrene	29.69	12.9	0.046	296.9
Indeno[1,2,3-cd]pyrene	31.75	1.1	0.046	317.5
Dibenz[a,h]anthracene	31.81	1.1	0.045	318.1
Benzo[ghi]perylene	32.19	8.4	0.046	321.9

Supelco EPA 502/524 Volatiles Organic Calibration Mix (without gasses)

Peaks	Retention Time (min)	Resolution	Peak Width (min)	Temperature (°C)
1,1-Dichloroethene	1.66	1.1	0.018	30
Dichloromethane	1.68	1.1	0.018	30
trans-1,2-Dichloroethene	1.86	2.1	0.02	30
1,1-Dichloroethane	1.9	2.1	0.021	30
cis-1,2-Dichloroethene	2.11	1.8	0.023	30
Bromochloromethane	2.15	1.7	0.024	30
2,2-Dichloropropane	2.19	--	0.024	30
Chloroform	2.19	--	0.024	30
1,2-Dichloroethane	2.46	3.5	0.027	30
1,1,1-Trichloroethane	2.56	3.5	0.029	30
1,1-Dichloropropene	2.71	1.7	0.03	30
Benzene	2.76	1.7	0.031	30
Carbon Tetrachloride	2.83	2.2	0.032	30
Dibromomethane	3.2	2.2	0.034	32.3
1,2-Dichloropropane	3.27	1.9	0.035	33.2
Bromodichloromethane	3.34	1.3	0.035	33.9
Trichloroethene	3.39	1.3	0.034	34.5
cis-1,3-Dichloropropene	3.98	11.9	0.034	41.3
trans-1,3-Dichloropropene	4.39	2.2	0.034	46
1,1,2-Trichloroethane	4.47	2.2	0.034	46.9
Toluene	4.67	0.7	0.034	49.2
1,3-Dichloropropane	4.7	0.7	0.034	49.5
Dibromochloromethane	4.94	5.3	0.034	52.3
1,2-Dibromoethane	5.12	5.3	0.034	54.3
Tetrachloroethene	5.51	11.6	0.034	58.9
Chlorobenzene	6.08	--	0.033	65.4
1,1,1,2-Tetrachloroethane	6.08	--	0.033	65.4

|			
Ethylbenzene	6.47	2	0.033	69.9
Bromoform	6.54	2	0.034	70.7
m-Xylene	6.64	0.6	0.033	71.9
p-Xylene	6.66	0.6	0.033	72.1
Styrene	6.95	2.3	0.033	75.4
1,1,2,2-Tetrachloroethane	7.03	1.2	0.033	76.3
o-Xylene	7.06	1.2	0.032	76.7
1,2,3-Trichloropropane	7.13	2.1	0.033	77.5
Bromobenzene	7.58	1.3	0.033	82.7
Isopropylbenzene	7.62	1.3	0.032	83.2
2-Chlorotoluene	8.01	3.3	0.032	87.6
4-Chlorotoluene	8.12	0.5	0.033	88.8
n-Propylbenzene	8.13	0.5	0.032	89
1,3,5-Trimethylbenzene	8.4	8.3	0.032	92.1
tert-Butylbenzene	8.77	0.3	0.032	96.4
1,2,4-Trimethylbenzene	8.79	0.3	0.032	96.5
1,3-Dichlorobenzene	8.85	1.8	0.032	97.2
1,4-Dichlorobenzene	8.93	2.5	0.033	98.2
sec-Butylbenzene	9.1	5.1	0.032	100.1
1,2-Dichlorobenzene	9.27	1	0.033	102.1
p-Isopropyltoluene	9.3	1	0.032	102.5
1,2-Dibromo-3-Chloropropane	9.75	0.3	0.033	107.6
n-Butylbenzene	9.76	0.3	0.032	107.7
1,2,4-Trichlorobenzene	11.32	3.4	0.033	125.6
Naphthalene	11.43	3.4	0.033	126.9
1,2,3-Trichlorobenzene	11.76	7.3	0.033	130.8
Hexachlorobutadiene	12.01	7.3	0.033	133.6

Appendix D

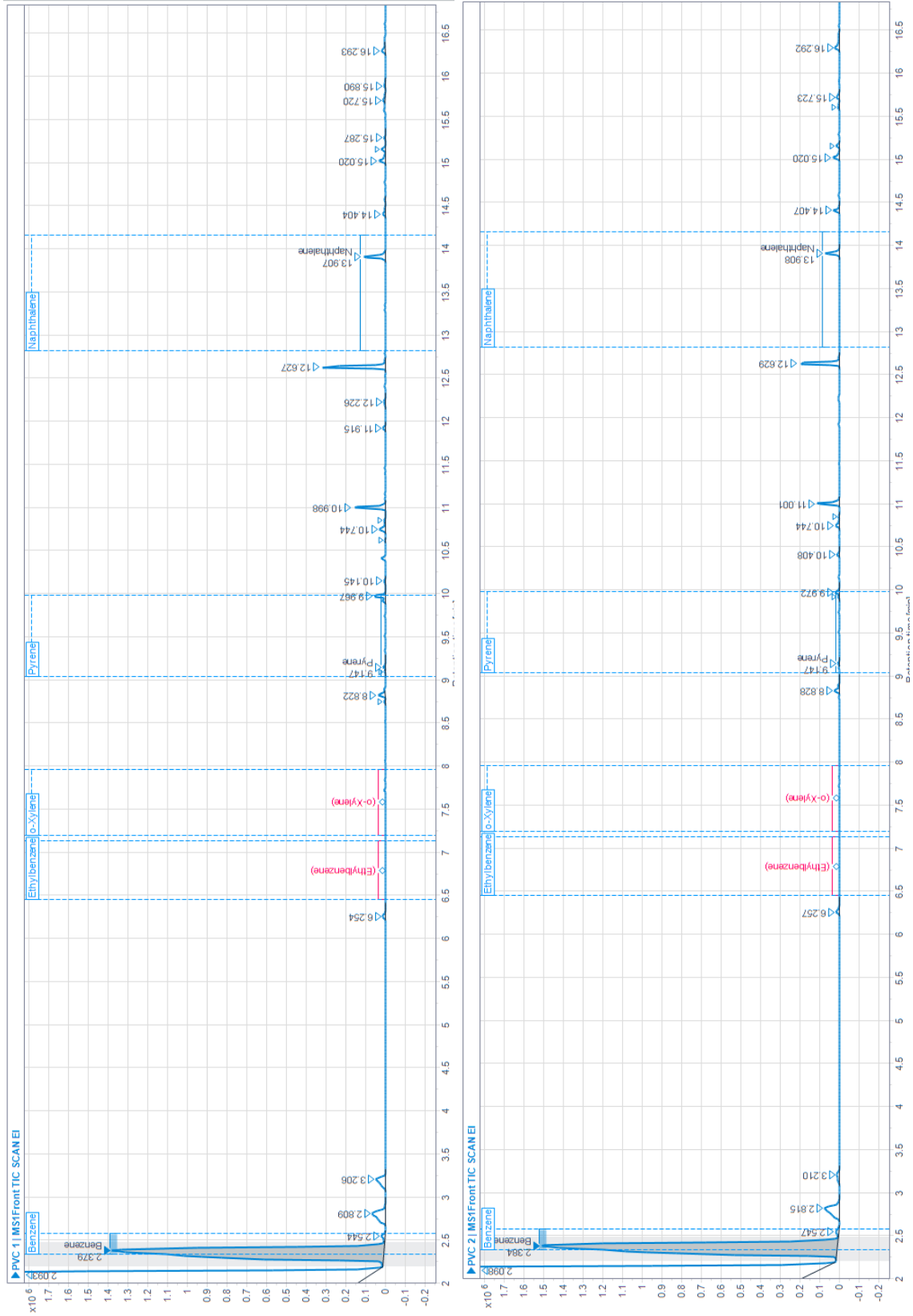GC-MS chromatograms for all eight samples

White Pine Samples
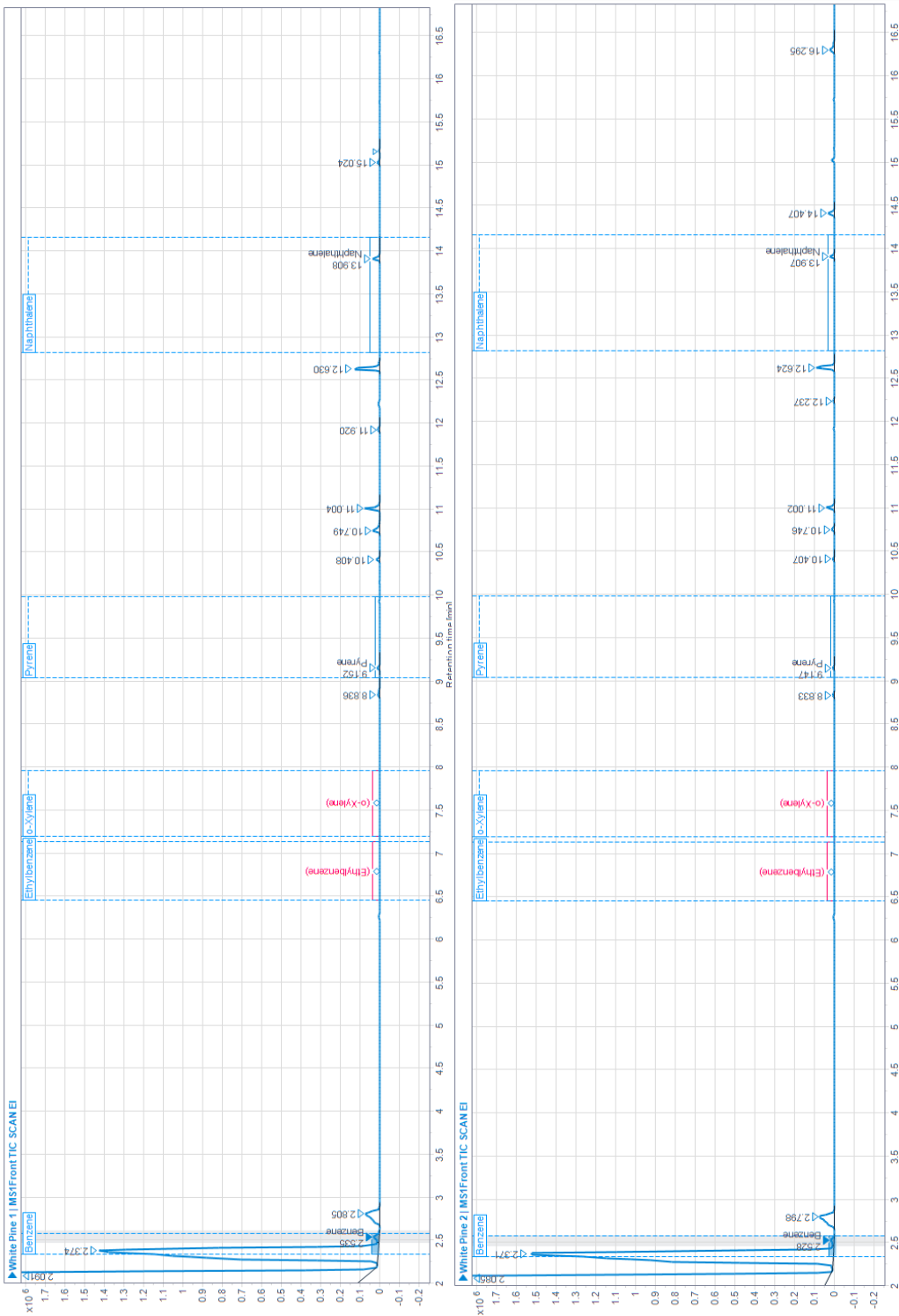
HDPE Samples
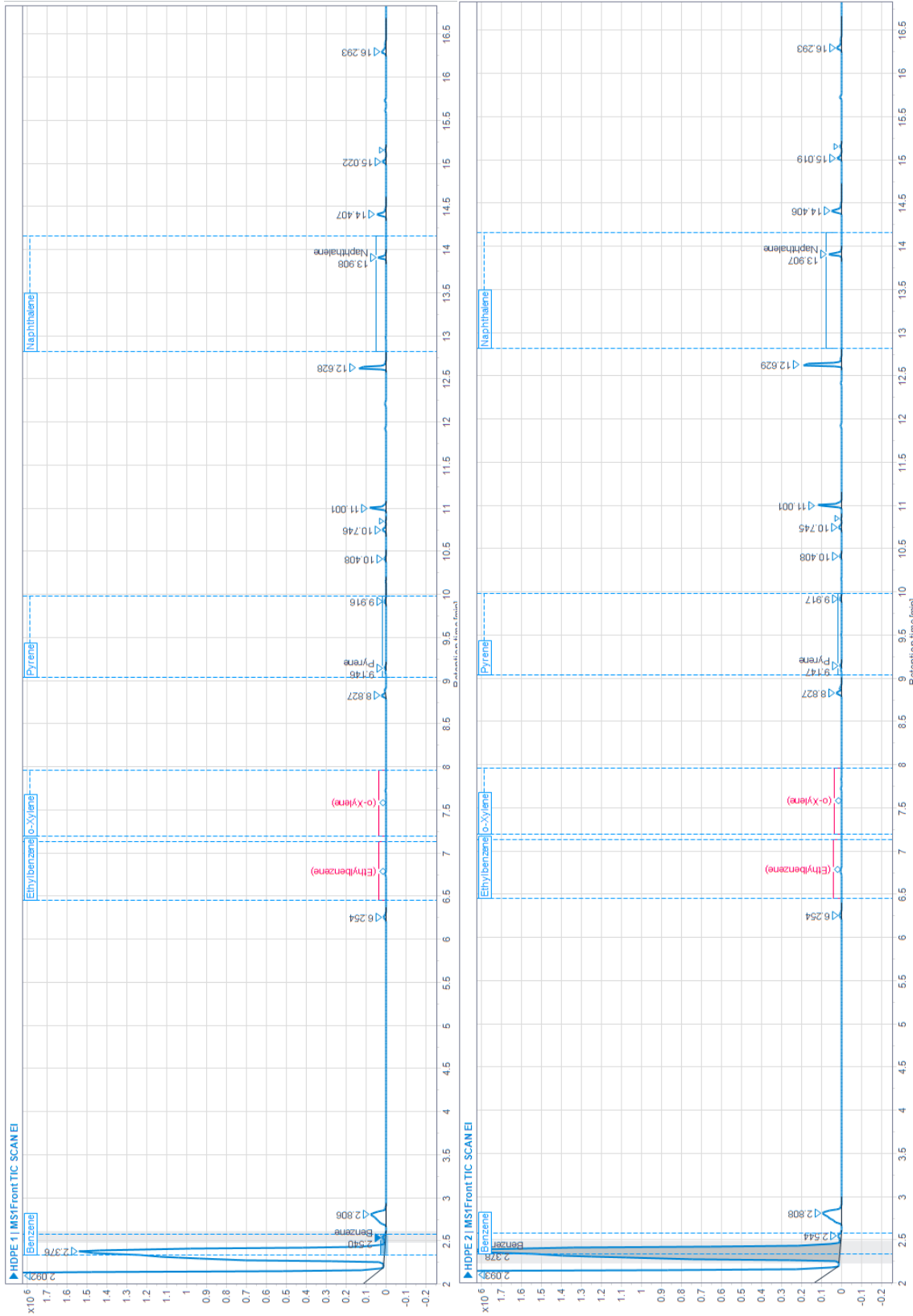
PVC Samples

Neoprene Rubber Samples

Appendix E

Potential Contaminants in Samples

Material	Burn #	Retention Time	Potential Contaminant	Probability	In literature
White Pine	1	2.091	n-Hexane	78.43	Yes
		2.805	Cyclohexane	66.4	No
		11.004	2-methoxyphenol	78.26	Yes
		12.63	Creosol	62.25	Yes
		15.158	2-methoxy-4-propylphenol	71.77	No
White Pine	2	1.952	3-methylpentane	67.2	No
		2.085	n-Hexane	78.73	Yes
		2.798	Cyclohexane	60.33	No
		10.407	2-methoxyphenol	60.71	Yes
		11.002	2-methoxyphenol	72.51	Yes
HDPE	1	2.092	n-Hexane	78.33	Yes
		2.806	Cyclohexane	67.12	No
		11.001	2-methoxyphenol	81.31	Yes
		15.157	2-methoxy-4-propylphenol	72.73	No
HDPE	2	2.093	n-Hexane	77.13	Yes
		2.544	Amylene Hydrate	83.81	No
		11.001	2-methoxy-phenol	76.55	Yes
		12.629	Creosol	61.4	Yes
		15.156	2-methoxy-4-propylphenol	73.73	No

		1.936	3-methylpentane	68.86	No
PVC	1	2.093	n-Hexane	77.99	Yes
		2.544	Amylene Hydrate	84.19	No
		8.747	Benzaldehyde	81.09	Yes
		9.967	2-ethyl-1-hexanol	63.56	Yes
		10.998	2-methoxyphenol	80.12	Yes
		15.156	2-methoxy-4-propylphenol	83.78	No
		2.098	n-Hexane	78.7	Yes
		2.547	Amylene Hydrate	75.31	No
PVC	2	9.972	2-ethyl-1-hexanol	66.72	Yes
		11.001	2-methoxyphenol	77.99	Yes
		15.155	2-methoxy-4-phenol	75.85	Yes
		19.072	4-hydroxy-3-methoxy-benzenepropanol	61.31	Yes
		2.103	n-Hexane	78.01	Yes
		2.552	Amylene hydrate	84	No
		2.818	Cyclohexane	64.35	No
		5.33	Cyclopentanone	69.97	No
		6.256	2-oxo-3-cyclopentene-1-acetaldehyde	67.38	No
Rubber	1	8.746	Benzaldehyde	64.91	Yes
		11	2-methoxy-phenol	77.91	Yes
		11.368	6,7-dihydro-5H-1-pyrindine	66.39	No
		13.132	Benzothiazole	66.66	No
		13.814	3-Ethyl-5,6,7,8-tetrahydroquinoline	65.98	No
		13.905	4-ethyl-2-methoxyphenol	76.99	No

		14.149	2-methyl-benzothiazole	74.42	Yes
		19.076	4-hydroxy-3-methoxy-benzenepropanol	77.81	Yes
		2.086	n-Hexane	78.61	Yes
		11.002	2-methoxy-phenol	62.69	Yes
		11.369	6,7-dihydro-5H-1-pyridine	74.87	No
Rubber	2	13.133	Benzothiazole	64.05	No
		13.907	4-ethyl-2-methoxyphenol	66.3	No
		14.151	2-methyl-benzothiazole	79.7	Yes